© 2020. Published by The Company of Biologists Ltd | Journal of Experimental Biology (2020) 223, jeb228114. doi:10.1242/jeb.228114

RESEARCH ARTICLE

Different microcircuit responses to comparable input from one versus both copies of an identified projection neuron

Gabriel F. Colton*, Aaron P. Cook* and Michael P. Nusbaum‡

ABSTRACT

Neuronal inputs to microcircuits are often present as multiple copies of apparently equivalent neurons. Thus far, however, little is known regarding the relative influence on microcircuit output of activating all or only some copies of such an input. We examine this issue in the crab (*Cancer borealis*) stomatogastric ganglion, where the gastric mill (chewing) microcircuit is activated by modulatory commissural neuron 1 (MCN1), a bilaterally paired modulatory projection neuron. Both MCN1s contain the same co-transmitters, influence the same gastric mill microcircuit neurons, can drive the biphasic gastric mill rhythm, and are co-activated by all identified MCN1-activating pathways. Here, we determine whether the gastric mill microcircuit response is equivalent when stimulating one or both MCN1s under conditions where the pair are matched to collectively fire at the same overall rate and pattern as single MCN1 stimulation. The dual MCN1 stimulations elicited more consistently coordinated rhythms, and these rhythms exhibited longer phases and cycle periods. These different outcomes from single and dual MCN1 stimulation may have resulted from the relatively modest, and equivalent, firing rate of the gastric mill neuron LG (lateral gastric) during each matched set of stimulations. The LG neuron-mediated, ionotropic inhibition of the MCN1 axon terminals is the trigger for the transition from the retraction to protraction phase. This LG neuron influence on MCN1 was more effective during the dual stimulations, where each MCN1 firing rate was half that occurring during the matched single stimulations. Thus, equivalent individual- and co-activation of a class of modulatory projection neurons does not necessarily drive equivalent microcircuit output.

KEY WORDS: Central pattern generator, Descending control, Gastric mill rhythm, Stomatogastric system

INTRODUCTION

Projection neurons that regulate microcircuit activity commonly occur as multiple copies of apparently equivalent neurons (Rosen et al., 1991; Blitz et al., 1999; Brodfuehrer and Thorogood, 2001; Hägglund et al., 2010; Betley et al., 2013; Bidaye et al., 2014; Gunaydin et al., 2014; Daghfous et al., 2016; Qiu et al., 2016; Li et al., 2017; Fino et al., 2018; Li and Soffe, 2019; Ruder and Arber, 2019). Although the consequences of their co-activation for microcircuit output and/or behavior are established in many systems, there appears to be no systematic comparison of a circuit response to co-activating all versus a defined subset of them. Such comparisons would help elucidate how these systems operate, and could inform whether continued normal behavior would be likely to occur after loss of some copies of a projection neuron due to injury or disease (Fink and Cafferty, 2016).

The microcircuit response to activating all or some copies of a projection neuron might be equivalent, particularly when those neurons act at least partly via peptide co-transmitters, because neurally released peptides diffuse broadly and have long-lasting effects on their targets (Marder, 2012; van den Pol, 2012; Nusbaum et al., 2017; Svensson et al., 2019). Alternatively, the microcircuit response might be skewed by the number of active projection neurons and their firing rates, for example because neuropeptide release often has a higher firing rate threshold than small molecule co-transmitters and its release can be a non-linear function of firing rate (Cazalis et al., 1985; Peng and Horn, 1991; Whim and Lloyd, 1994; Vilim et al., 1996, 2000; Arrigoni and Saper, 2014; Nusbaum et al., 2017), and modulatory actions can be concentration specific (Flamm and Harris-Warrick, 1986; Saideman et al., 2006; Fort et al., 2007; Poels et al., 2007, 2009; Dickinson et al., 2015; Blitz et al., 2019). There is also the additional challenge of establishing whether an apparently equivalent set of projection neurons are indeed functionally equivalent. In some cases, such sets of neurons were subsequently determined to diverge and influence overlapping or distinct sets of neurons (Lammel et al., 2011; Betley et al., 2013; Luo et al., 2018). There can also be distinct responses to activating all versus some copies of a projection neuron when they are bilaterally symmetrical and normally operate separately to mediate hemilateral movements (Shimazaki et al., 2019; Cregg et al., 2020).

Manipulating the activity of multiple copies of a projection neuron in a controlled manner is possible, for example by optogenetics, but it remains challenging to precisely manipulate a defined subset of them. Such precision is possible, however, in some smaller systems where identified projection neurons with a known influence on a target microcircuit are present as small copy numbers (Rosen et al., 1991; Frost and Katz, 1996; Blitz et al., 1999; Brodfuehrer and Thorogood, 2001; Mesce et al., 2008; Jeanne and Wilson, 2015).

One tractable system for such a study is the stomatogastric nervous system (STNS) of the crab *Cancer borealis* (Marder and Bucher, 2007; Daur et al., 2016; Nusbaum et al., 2017; Stein, 2017). This system contains two well-characterized microcircuits in the stomatogastric ganglion (STG) that generate the motor patterns for chewing (gastric mill microcircuit), and the pumping and filtering of chewed food (pyloric microcircuit) *in vivo* and in the isolated STNS. These circuits are readily accessible in the isolated STNS because most of the 26 STG neurons contribute to one or both of these microcircuits, their somata are relatively large (diameter ~35–120 µm), and most microcircuit neurons occur as single copies (Marder et al., 2017). There are also six different identified

Department of Neuroscience, 211 Clinical Research Building, 415 Curie Boulevard, Perelman School of Medicine, University of Pennsylvania, Philadelphia, PA 19104, USA.

*These authors contributed equally to this work

‡Author for correspondence (nusbaum@pennmedicine.upenn.edu)

G.F.C., 0000-0002-3690-1586; M.P.N., 0000-0001-5935-0046

Received 1 May 2020; Accepted 13 August 2020

Journal of Experimental Biology (2020) 223, jeb228114. doi:10.1242/jeb.228114

List of symbols and abbreviations

AGR	anterior gastric receptor (neuron)
AM	anterior median (neuron)
CabTRP Ia	*Cancer borealis* tachykinin-related peptide Ia
CoG	commissural ganglion
DCC	discontinuous current clamp
DG	dorsal gastric (neuron)
dgn	dorsal gastric nerve
dpon	dorsal posterior oesophageal nerve
dvn	dorsal ventricular nerve
GABA	gamma aminobutyric acid
GM	gastric mill (neuron)
G_{MI}	modulator-activated voltage-dependent inward conductance
IC	inferior cardiac (neuron)
I_{MI}	modulator-activated inward current
Int1	interneuron 1
ion	inferior oesophageal nerve
LG	lateral gastric (neuron)
lgn	lateral gastric nerve
ln	labral nerve
lvn	lateral ventricular nerve
MCN1	modulatory commissural neuron 1
$MCN1_L$	left MCN1
$MCN1_R$	right MCN1
$MCN1_{STG}$	STG terminals of MCN1
MCN5	modulatory commissural neuron 5
MG	medial gastric (neuron)
mvn	medial ventricular nerve
PD	pyloric dilator (neuron)
pdn	pyloric dilator nerve
son	superior oesophageal nerve
STG	stomatogastric ganglion
stn	stomatogastric nerve
STNS	stomatogastric nervous system
VCNs	ventral cardiac neurons
VD	ventricular dilator (neuron)

projection neuron pairs that regulate gastric mill and/or pyloric circuit activity (Coleman et al., 1992; Norris et al., 1994, 1996; Blitz et al., 1999; Christie et al., 2004).

The best characterized projection neuron in the *C. borealis* STNS is modulatory commissural neuron 1 (MCN1) (Coleman and Nusbaum, 1994; Hedrich et al., 2011; Nusbaum et al., 2017). Each MCN1 projects an axon from one of the paired commissural ganglia (CoGs), through the inferior oesophageal nerve (*ion*) and stomatogastric nerve (*stn*), to innervate the STG and drive the gastric mill and pyloric rhythms (Coleman et al., 1992; Coleman and Nusbaum, 1994; Bartos and Nusbaum, 1997). MCN1 can be selectively driven by extracellular *ion* stimulation, and both MCN1s contain the same co-transmitters, influence the same STG circuit neurons, and drive the gastric mill rhythm by the same mechanism (Coleman et al., 1995; Bartos and Nusbaum, 1997; Bartos et al., 1999; Blitz et al., 1999; Wood et al., 2000; Stein et al., 2007; DeLong et al., 2009a,b; Nusbaum et al., 2017). Furthermore, despite being present in separate ganglia, both MCN1s are co-activated by all identified sensory and central nervous system (CNS) pathways (Beenhakker et al., 2004, 2005; Blitz et al., 2004, 2008; Christie et al., 2004; Hedrich et al., 2009; Blitz and Nusbaum, 2012; White et al., 2017).

Here, we examine whether the gastric mill microcircuit response to dual and single MCN1 stimulation, in preparations where the CoGs are removed and the MCN1 axon in the *ion* is selectively stimulated, is comparable when the two conditions have matched firing rates and patterns. We ensure this match by co-stimulating the two MCN1s in a one-to-one alternating pattern that produces an inter-stimulus interval equivalent to that used for the matched single MCN1 stimulation. These matched stimulations did not elicit equivalent gastric mill rhythms. For example, the gastric mill rhythm was more consistently coordinated during the dual MCN1 stimulations. These different outcomes likely resulted at least partly from the similar firing frequency of the gastric mill rhythm generator neuron LG (lateral gastric) across each set of matched single and dual MCN1 stimulations. This similar LG neuron activity was likely more effective in inhibiting each MCN1 during the dual stimulations, where their firing frequency was half that of the same neuron in the corresponding single stimulation. These results indicate that at least some neural circuits are optimally driven by co-activating all copies of circuit-driving projection neurons.

MATERIALS AND METHODS

Animals

Adult male Jonah crabs (*Cancer borealis* Stimpson 1859) were obtained from commercial suppliers (Fresh Lobster, LLC; Marine Biological Laboratory; Ocean Resources, Inc.) and maintained in aerated, filtered artificial seawater at 10–12°C. Animals were cold anesthetized by packing in ice for at least 30 min before dissection. The foregut was then removed from the animal, after which the STNS was dissected from the foregut in physiological saline at 4°C. The dorsal connective tissue sheath of the STG was removed immediately prior to recording to facilitate access for intrasomatic recordings.

Solutions

Cancer borealis physiological saline contained the following (mmol l^{-1}): 440 NaCl, 26 $MgCl_2$, 13 $CaCl_2$, 11 KCl, 10 Trizma base, 5 maleic acid and 5 glucose; pH 7.4–7.6. All preparations were superfused continuously with *C. borealis* saline (8−12°C).

Electrophysiology

Electrophysiology experiments were performed using standard techniques for this system (Beenhakker and Nusbaum, 2004). The isolated STNS (Fig. 1A) was pinned down in a silicone elastomer-lined (Sylgard 184, KR Anderson) Petri dish. Each extracellular nerve recording resulted from a pair of stainless-steel wire electrodes (reference and recording) whose ends were pressed into the Sylgard-coated dish. A differential AC amplifier (model 1700, A-M Systems) amplified the voltage difference between the reference wire (placed in the bath) and the recording wire [placed near an individual nerve and isolated from the bath by petroleum jelly (Vaseline, Lab Safety Supply)]. This signal was then further amplified and filtered (model 410 amplifier, Brownlee Precision). Extracellular nerve stimulation was accomplished by placing the pair of wires used to record nerve activity into a stimulus isolation unit (SIU 5, AstroNova Inc.) that was connected to a stimulator (model S88, AstroNova Inc.).

Intrasomatic recordings were made with sharp glass microelectrodes (8–20 MΩ) filled with potassium acetate (4 mol l^{-1}) plus KCl (20 mmol l^{-1}), or KCl alone (1 mol l^{-1}). Intracellular signals were amplified using Axoclamp 2B amplifiers (Molecular Devices), and then further amplified and filtered (model 410 amplifier). Current injections were performed in single-electrode discontinuous current-clamp (DCC) mode with sampling rates between 2 and 3 kHz. To improve visibility for intracellular recording, the STG was dorsally desheathed and viewed with light transmitted through a

Journal of Experimental Biology (2020) 223, jeb228114. doi:10.1242/jeb.228114

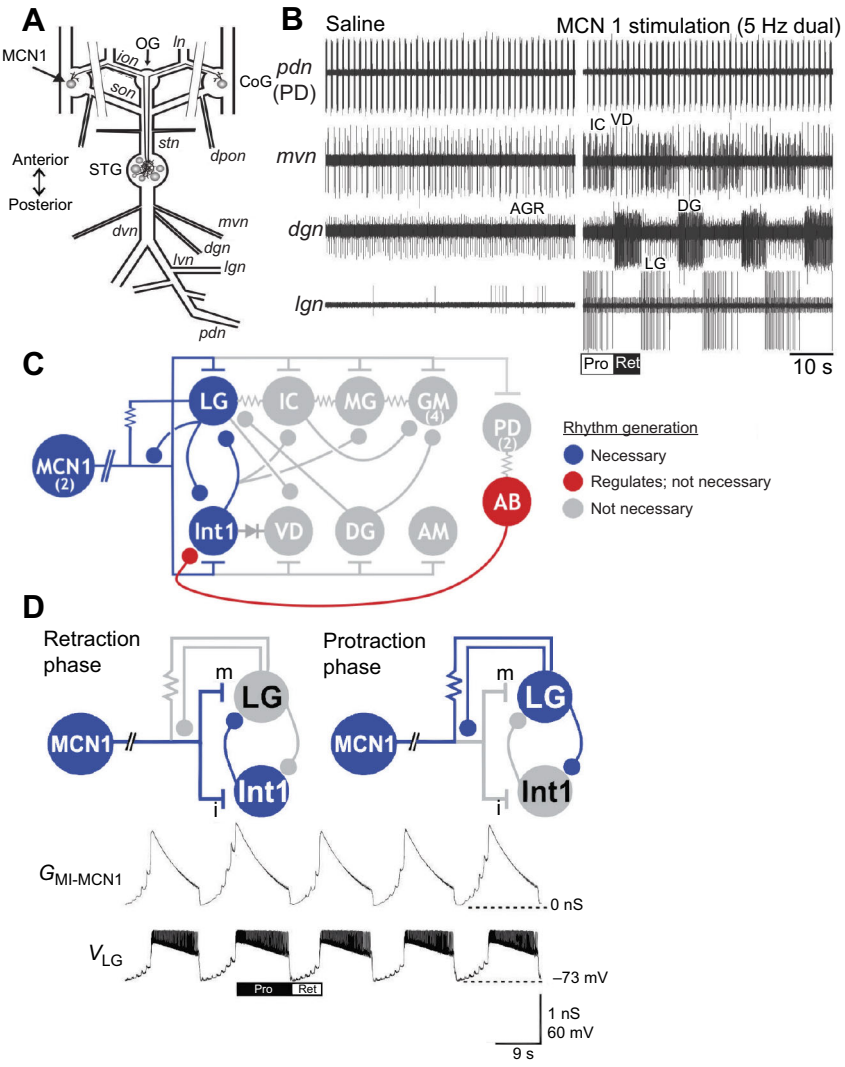

Fig. 1. The projection neuron MCN1 drives the gastric mill rhythm in the isolated stomatogastric nervous system of the crab *Cancer borealis*. (A) STNS schematic, with the parallel lines crossing the *ion*s and *son*s representing the nerve transections used to remove the CoGs. OG, oesophageal ganglion; STG, stomatogastric ganglion. (B) Selective MCN1 (*ion*) stimulation drives the gastric mill rhythm. Before stimulation ('Saline'), there was an ongoing pyloric rhythm [pyloric dilator nerve (*pdn*), *mvn* (medial ventricular nerve)] but no gastric mill rhythm [dorsal gastric nerve (*dgn*), lateral gastric nerve (*lgn*)]. Small unit in *mvn*: GM neurons; small continuously present units in the *lgn* are stimulation artifacts (SA). The AGR (anterior gastric receptor) is a sensory neuron that only influences the gastric mill rhythm via its actions in the CoGs (Simmers and Moulins, 1988; Norris et al., 1994; Smarandache and Stein, 2007; Hedrich et al., 2009). Pro, protraction; Ret, retraction. (C) Schematic of the MCN1-driven gastric mill microcircuit. Top row, protractor neurons; bottom row, retractor neurons. Labels: filled circles, inhibition; T-bars, excitation; resistors, non-rectifying electrical coupling; diode, rectified electrical coupling; double slashed lines on MCN1 axon, space break. Modified from Saideman et al. (2007). (D) Top: schematic of the phase-specific operation of the MCN1–gastric mill rhythm generator circuit. Labels: blue, active neurons and synapses; grey, inactive neurons and synapses. Bottom: computational model output of the MCN1–gastric mill rhythm activity in the LG neuron plus the associated, rhythmic waxing and waning of MCN1-activated G_{MI} in LG ($G_{MI\text{-}MCN1}$). m, metabotropic transmission; i, ionotropic transmission. Modified from DeLong et al. (2009b).

dark-field condenser (Nikon). STG neurons were identified on the basis of their axonal projections, activity patterns and interactions with other STG neurons (Weimann et al., 1991; Blitz et al., 2008). In the displayed extracellular nerve recordings, all action potentials of a given amplitude in a particular nerve are generated by the neuron indicated above a subset of those action potentials (Nusbaum et al., 2017).

Each *ion* was stimulated (duration per stimulus: 1 ms), just medial to the labral nerve (*ln*; Fig. 1A), to selectively activate the left MCN1 ($MCN1_L$) or the right MCN1 ($MCN1_R$) (Bartos and Nusbaum, 1997). The left and right CoG, and hence $MCN1_L$ and $MCN1_R$, were defined based on the isolated STNS being pinned with the dorsal side facing up. There is only one other CoG projection neuron (MCN5) that innervates the STG which has an axon in the *ion*, and it has a higher stimulus threshold than MCN1 as well as having no direct influence on LG (Coleman et al., 1992; Norris et al., 1996; Blitz et al., 2019). Each suprathreshold *ion* stimulus elicited a single MCN1 action potential, as established by recording the resulting unitary, electrical excitatory postsynaptic potential (EPSP) in the LG neuron (Coleman et al., 1995). Using a voltage setting on the stimulator that was ≤0.5 V above threshold for eliciting MCN1 action potentials prevented or minimized co-stimulation of MCN5 (Bartos and Nusbaum, 1997). A tonic *ion* stimulation pattern (i.e. constant inter-stimulus intervals) was used in all these experiments.

To determine the relative influence of matched dual versus single MCN1 stimulation on the gastric mill rhythm, we used a range of MCN1 firing rates that spanned its activity range in response to input pathway stimulation. Specifically, we stimulated each MCN1 separately, at 10, 20 or 30 Hz using a tonic stimulation pattern. We compared these single stimulations to matched dual MCN1 stimulation during which the two MCN1s were each stimulated at 50% of the firing rate of the associated single stimulations (e.g. 5 Hz+5 Hz compared with 10 Hz). During dual stimulation, each MCN1 was activated to fire a single action potential alternately, such that their combined firing rate and pattern was the same as the matched single stimulation. To ensure the occurrence of the same MCN1 inter-spike interval during the matched single and dual MCN1 stimulations, we consistently tracked the presence of MCN1-evoked EPSPs in the intracellular LG neuron recordings.

In some experiments where the activity of the retraction phase neuron DG (dorsal gastric) persisted through the protraction phase of the gastric mill rhythm, the ability of the protractor neuron LG to regulate DG activity was examined by injecting LG with suprathreshold depolarizing current pulses during some of its bursts to increase its within-burst firing rate. In these same experiments, we also determined the impact of these LG current injections on the pyloric cycle period (see below). The LG current injections (+1 to +4 nA) were done in DCC, using brief

depolarizing pulses (pulse duration: 30–50 ms) that each elicited a single action potential. Each within-burst current injection train was turned on and off manually, and was timed to occur during a normal LG burst for a duration similar to the LG burst duration during that particular gastric mill rhythm. These manipulations were performed in a subset of experiments during dual 10 Hz and single 20 Hz MCN1 stimulated gastric mill rhythms. Two of these LG current injections, separated by four to eight control LG bursts, were performed during each gastric mill rhythm.

In control experiments, the mechanosensory ventral cardiac neurons (VCNs) were activated by stimulating the dorsal posterior oesophageal nerve (*dpon*; duration per stimulus: 1 ms), either unilaterally or bilaterally, in preparations where the superior oesophageal nerves (*son*s) were bisected between the *dpon* and the *stn*. The VCNs innervate the ipsilateral CoG via the *dpon* and *son*, and their stimulation triggers a version of the gastric mill rhythm by eliciting a long-lasting activation of the CoG projection neurons MCN1 and CPN2 (commissural projection neuron 2) (Beenhakker et al., 2004; Beenhakker and Nusbaum, 2004). Bisecting the *son*s, through which the CPN2 axon projects to the STG, prevents CPN2 activity from influencing the STG, enabling VCN stimulation to influence the gastric mill microcircuit exclusively via its activation of MCN1 (Norris et al., 1994; Beenhakker and Nusbaum, 2004). These experiments included both bilateral (N=2) and unilateral VCN stimulations (N=3). In each experiment, the MCN1 firing rate resulting from VCN stimulation was determined on the stimulated side(s) and subsequently used as the ipsilateral *ion* stimulation frequency, to compare the gastric mill rhythm response to direct (*ion* stimulation) and indirect (*dpon* stimulation) activation of MCN1. All *ion* stimulation experiments were performed from September 2013 to March 2015. The *dpon* versus *ion* stimulation experiments were performed during February and March 2017.

Data analysis

Data were collected in parallel onto a chart recorder (AstroNova Everest model) and computer. Acquisition onto computer (sampling rate ∼5 kHz) used the Spike2 data acquisition and analysis system (Cambridge Electronic Design). Some analyses, including cycle period, burst durations, duty cycle, number of action potentials per burst and intraburst firing frequency were conducted on the digitized data using a custom-written Spike2 program (‘The Crab Analyzer’). To facilitate data analysis and improve clarity in some figures, a raw extracellular recording (e.g. dorsal gastric nerve, *dgn*) was duplicated with the stimulation artifacts digitally subtracted, reducing their amplitude or eliminating them. This is indicated where appropriate in each figure legend, and is illustrated in Fig. 2B. A custom-written script in Spike2 was used to digitally subtract the artifacts after manually inspecting the trace to verify that only that particular unit was selected for subtraction (Blitz and Nusbaum, 2008).

Unless otherwise stated, each data point in a dataset was derived by determining the mean for the analysed parameter from 8–20 consecutive gastric mill cycles. One gastric mill cycle was defined as extending from the onset of consecutive LG neuron action potential bursts (Beenhakker and Nusbaum, 2004; Wood et al., 2004). Thus the gastric mill cycle period was measured as the duration between the onset of two successive LG neuron bursts. The protractor phase was measured as the LG burst duration, whereas the retractor phase was measured as the LG interburst duration. A gastric mill rhythm-timed burst duration was defined as the duration between the onset of the first and last action potential within an impulse burst, during which no interspike interval was longer than 2 s (approximately twice the pyloric cycle period during the gastric mill rhythm and no more than half the duration of each gastric mill phase) (Beenhakker et al., 2004). The intraburst firing rate of a neuron was defined as the number of action potentials within a burst minus one, divided by the burst duration. The pyloric cycle period was determined as the duration between the onset of successive bursts in the pyloric dilator (PD) neuron (Fig. 1B). The PD neuron is a pyloric pacemaker neuron component (Marder and Bucher, 2007; Selverston and Miller, 1980).

To evaluate the influence of the LG neuron depolarizing current injections on the pyloric cycle period, the longest pyloric cycle that occurred after the start of the LG burst was selected for analysis during (a) each LG burst that received depolarizing current pulses, and (b) the two preceding LG bursts. The first pyloric cycle after LG burst onset was always the slowest one (i.e. longest cycle period) during the control LG bursts and was the slowest during 77% of the depolarized LG bursts, likely reflecting the fact that the LG instantaneous firing rate was often highest at the start of its burst. To compare these pyloric cycle periods between the depolarized and control LG bursts, we first determined and compared the ratios of the pyloric cycle period from the (a) depolarized LG burst divided by that from the preceding control LG burst, and (b) the same preceding control LG burst divided by that from the control LG burst two prior to the depolarized burst.

Data were plotted with Excel (version 2002; Microsoft) and MATLAB (version 8; MathWorks). Figures were produced using CorelDraw (version 13.0 for Windows). Statistical analyses were performed by comparing the overall mean of individual mean values for two different manipulated conditions, or control and manipulated groups, from N experiments (see Results for each N value) using Microsoft Excel, SigmaPlot 13.0 (SPSS Inc.) and MATLAB. Unless otherwise indicated, the presented N values represent the number of preparations. Comparisons were made to determine statistical significance using (a) repeated-measures ANOVA (RM-ANOVA), with the Holm–Šidák *post hoc* test when the RM-ANOVA P-value was <0.05, (b) RM-ANOVA on ranks, with *post hoc* Tukey’s test or chi-square test, (c) paired Student’s t-test, (d) signed rank test, (e) chi-square test (different from the aforementioned *post hoc* chi-square test), (f) Fisher’s exact test, (g) Wilcoxon signed rank test or (h) unpaired t-test. In all experiments, the effect of each manipulation was reversible, and there was no significant difference between the pre- and post-manipulation groups. Significant differences were determined to occur when P<0.05. Data are expressed as means±s.e.m.

RESULTS

The gastric mill rhythm is a two-phase motor pattern (protraction, retraction) that drives the rhythmic contraction of striated muscles in the middle (i.e. gastric mill) stomach compartment of decapod crustaceans (Heinzel, 1988; Heinzel et al., 1993; Diehl et al., 2013). The sequence of these muscle contractions causes the paired lateral teeth and medial tooth within the gastric mill to rhythmically move towards (protract) and away from (retract) the midline, macerating food moved into the gastric mill from the anterior, cardiac sac stomach compartment. The chewed food is then filtered and pumped through the posterior stomach compartment, the pylorus, to enter the midgut for nutrient absorption. The rhythmic chewing pattern is generated by the gastric mill central pattern generator circuit, an episodically active microcircuit in the STG that is driven by projection neurons, including the paired MCN1s, located in the CoGs (Fig. 1A,C) (Coleman and Nusbaum, 1994;

Journal of Experimental Biology (2020) 223, jeb228114. doi:10.1242/jeb.228114

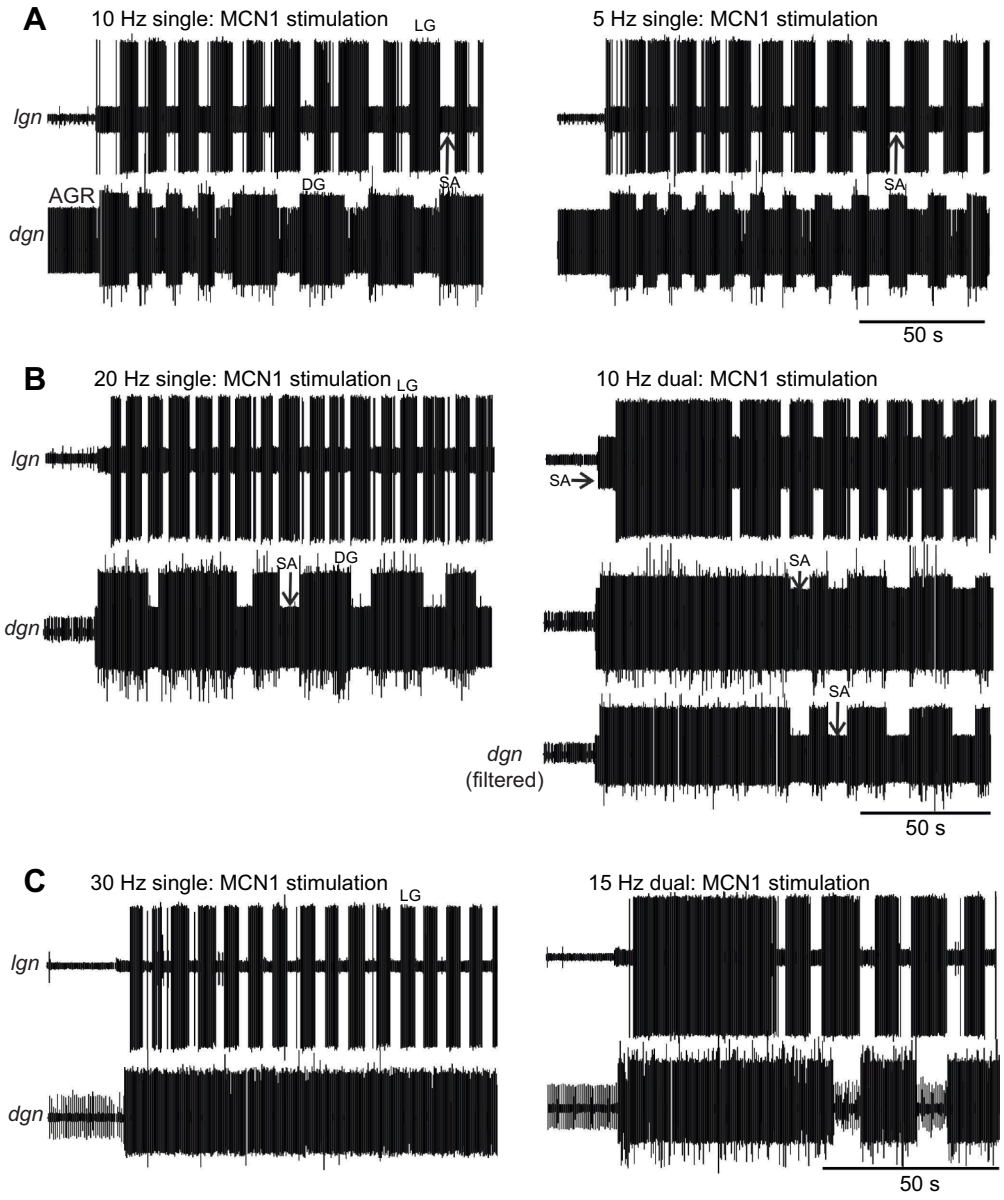

Fig. 2. Example recordings of gastric mill rhythms in response to firing rate- and pattern-matched dual and single MCN1 stimulations on a compressed time scale. Each rhythm is represented by extracellular recordings of the protractor LG (*lgn*) and retractor DG (*dgn*) neurons. Thickened baseline represents stimulation artifacts (SA). AGR, anterior gastric receptor (neuron). Each matched pair comes from the same experiment, but the different panels come from different experiments. Where noted in this and succeeding figures, nerve recordings were filtered to digitally reduce SA size to better separate them from the recorded action potentials. (A) 5 Hz dual versus 10 Hz single MCN1 stimulation. (B) 10 Hz dual versus 20 Hz single MCN1 stimulation, including *dgn* without versus with filtering in the '10 Hz dual' panel. (C) 15 Hz dual versus 30 Hz single MCN1 stimulation. Filtered *dgn*: all recordings except 20 Hz single stimulation.

Bartos et al., 1999; Beenhakker and Nusbaum, 2004; Blitz et al., 2008, 2019). The gastric mill rhythm is episodically active, *in vivo* and *in vitro*, because the projection neurons that drive it are episodically active, requiring excitatory drive from sensory neurons and other CNS neurons (Beenhakker et al., 2004; Blitz et al., 2004, 2008; Christie et al., 2004; Hedrich et al., 2009, 2011; Diehl et al., 2013).

There are eight gastric mill microcircuit neuron types, including four protractor motor neurons [LG, MG, GM (gastric mill), IC (inferior cardiac)] and four retraction phase neurons [one interneuron: Int1; three motor neurons: DG, VD (ventricular dilator), AM (anterior median)] (Fig. 1C) (Nusbaum et al., 2017). All but GM are present as single copies; there are four GMs. The neurons that are necessary and sufficient to generate the gastric mill rhythm (i.e. the rhythm-generating sub-circuit) during selective MCN1 activation includes the reciprocally inhibitory pair LG–Int1 plus the STG terminals of MCN1 ($MCN1_{STG}$) (Fig. 1D) (Coleman et al., 1995; Bartos et al., 1999; DeLong et al., 2009b; Nusbaum et al., 2017).

MCN1 is a multi-transmitter neuron that uses only its peptide co-transmitter CabTRP Ia (*Cancer borealis* tachykinin-related peptide Ia) to influence LG, causing a slowly developing metabotropic excitation by activating I_{MI} (modulator-activated inward current), while it uses only its small molecule co-transmitter GABA to influence Int1, causing a fast ionotropic excitation (Blitz et al., 1999; Wood et al., 2000; Stein et al., 2007). I_{MI} is a voltage-dependent depolarizing current with NMDA-like properties that is activated in STG neurons by many neuromodulators (Golowasch and Marder, 1992; Swensen and Marder, 2000, 2001; DeLong et al., 2009b; Rodriguez et al., 2013). MCN1 also has a functionally important electrical synapse with LG which strengthens the LG burst (Coleman et al., 1995). The MCN1 transmitter-mediated actions are limited to the retraction phase, because it receives fast glutamatergic inhibition at its STG terminals during protraction from LG (Coleman and Nusbaum, 1994). This LG-mediated inhibition triggers the transition from retraction to protraction and, by triggering decay of I_{MI} amplitude, enables the eventual transition from protraction to retraction (Fig. 1D) (Coleman et al., 1995;

Journal of Experimental Biology (2020) 223, jeb228114. doi:10.1242/jeb.228114

DeLong et al., 2009b). Here, we use the LG neuron burst to represent the protraction phase, and the LG neuron interburst burst to represent the retraction phase (Fig. 1B).

Distinct LG and DG neuron coordination during dual versus single MCN1 stimulation

We determined how consistently fully coordinated gastric mill rhythms were generated from three sets of matched dual versus single MCN1 stimulations (5 Hz dual versus 10 Hz single; 10 Hz dual versus 20 Hz single; 15 Hz dual versus 30 Hz single) (Fig. 3). A fully coordinated gastric mill rhythm exhibits consistent alternating bursting between the protraction- and retraction-phase neurons (Fig. 1B,C). Most aspects of this patterning during the MCN1-driven gastric mill rhythm result directly from the microcircuit synapses made by the rhythm generator neurons LG and Int1 (Fig. 1C) (Bartos et al., 1999; White and Nusbaum, 2011). Consequently, most gastric mill neuron activity is tightly linked to that of LG and/or Int1. For example, IC neuron activity is consistently limited to the protraction phase while VD neuron activity is limited to the retraction phase (Figs 1B and 4). In contrast, the gastric mill rhythm-timed bursting pattern of the retractor neuron DG is an indirect consequence of LG neuron activity. Specifically, the DG neuron burst pattern results from the LG ionotropic inhibition of $MCN1_{STG}$, which weakens or eliminates MCN1 metabotropic excitation of DG (Fig. 1C,D) (Coleman and Nusbaum, 1994). As is evident in Fig. 2, in our matched MCN1 stimulation experiments DG neuron activity was not always limited to the retraction phase.

As shown in Fig. 3, fully coordinated gastric mill cycles occurred more consistently during 5 Hz dual MCN1 stimulation than 10 Hz single stimulation (fraction of coordinated cycles per gastric mill rhythm: 5 Hz dual, 0.91±0.08; 10 Hz_R single, 0.47±0.11; 10 Hz_L single, 0.45±0.11; RM-ANOVA, $P<0.001$; Holm–Šidák *post hoc* test: 5 Hz dual versus 10 Hz_R or 10 Hz_L, $P=0.001$; 10 Hz_R versus 10 Hz_L, $P=0.90$; $N=10$ preparations). Additionally, in eight of the 10 (80%) 5 Hz dual stimulation experiments, there was LG and DG burst alternation in every gastric mill rhythm cycle (Fig. 3). In contrast, a fully coordinated gastric mill rhythm occurred in only one of 10 (10%) experiments each for the 10 Hz_L and 10 Hz_R single stimulations (Fig. 3).

In contrast to the 5 Hz dual–10 Hz single stimulations, there was no difference in the mean fraction of gastric mill cycles exhibiting LG–DG alternation during the two higher matched pairs of MCN1 stimulation (10 Hz dual, 0.47±0.12; 20 Hz_L single, 0.29±0.13; 20 Hz_R single, 0.15±0.05; RM-ANOVA, $P=0.09$, $N=11$ preparations; 15 Hz dual, 0.36±0.14; 30 Hz_L single, 0.23±0.01; 30 Hz_R single, 0.06±0.05, RM-ANOVA, $P=0.1$, $N=11$) (Fig. 3). However, the median values of the 10 Hz dual and 20 Hz single matched pairs were offset considerably, due in part to there being a higher percentage of rhythms with no cycles of LG–DG alternation during the single stimulations [20 Hz single, 10/22 (45%); 10 Hz dual, 2/11 (18%); Fig. 3]. This difference was also present, albeit to a lesser degree, for the highest matched stimulations [30 Hz single, 15/22 (68%); 15 Hz dual, 6/11 (55%); Fig. 3].

There was also separation between the 10 Hz dual–20 Hz single MCN1 stimulations with respect to the percentage of experiments in which more than half of the cycles displayed LG–DG alternation (10 Hz dual, $N=6/11$, 55%; 20 Hz single: $N=3/22$, 14%; $P=0.033$, Fisher's exact test), but this was not the case for the 15 Hz dual–30 Hz single stimulations ($P=0.186$) (Fig. 3). However, unlike the consistently coordinated gastric mill rhythms that occurred during the dual 5 Hz stimulations, comparable full coordination for all cycles only occurred during two of 11 preparations (18%) for both 10 Hz dual and 15 Hz dual stimulations (Fig. 3). During the single MCN1 stimulations, full coordination during all cycles occurred in only two of 20 (10%) 10 Hz stimulations, two of 22 (9.1%) 20 Hz stimulations, and none of the 30 Hz ($N=22$) stimulations. Across all three sets of matched MCN1 stimulations, at least 50% of cycles exhibited LG–DG burst alternation in more of the dual (19/32; 59%) than the single (19/64; 30%) stimulations ($P=0.01$, chi-square test on contingency table).

During gastric mill rhythm cycles when LG–DG burst alternation did not occur, DG neuron activity persisted through the LG burst (Figs 2 and 4). When DG activity did continue through the protraction phase, its firing rate was consistently reduced relative to that during retraction (10 Hz single: $P<0.001$, $N=9$; 10 Hz dual: $P=0.002$, $N=5$; 20 Hz single: $P<0.001$, $N=10$; 15 Hz dual: $P=0.015$, $N=4$; 30 Hz single: $P=0.008$*, $N=8$; paired *t*-test, except *signed rank test). This DG firing rate reduction during protraction was greater during the dual 10 Hz and dual 15 Hz MCN1 stimulations

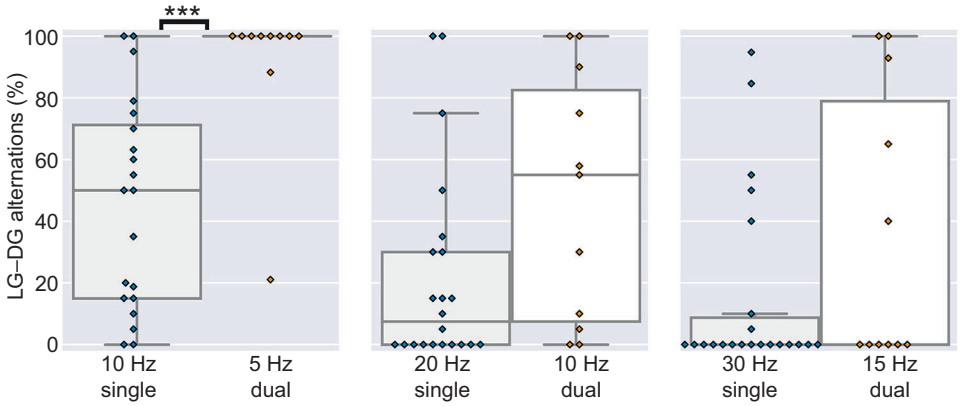

Fig. 3. Percentage of gastric mill rhythm cycles exhibiting alternating LG and DG neuron bursts during matched dual and single MCN1 stimulation. Box and whisker plots display the percentage of cycles per gastric mill rhythm during which the LG and DG neurons burst in alternation during each pair of matched MCN1 stimulations. Bottom and top of each box represents the first and third quartile for each data set, respectively, while the 'whiskers' extend to 1.5× the interquartile range. The horizontal line within each box indicates the median value; filled diamonds indicate the mean value per experiment. Note that due to the data distribution, the box and whiskers are collapsed into a single line for the 5 Hz dual stimulation data set, as are the first quartile, median and whisker labels for the 15 Hz dual condition. Statistical analysis: RM-ANOVA, Holm–Šidák *post hoc* test: ***$P\leq0.001$.

Journal of Experimental Biology (2020) 223, jeb228114. doi:10.1242/jeb.228114

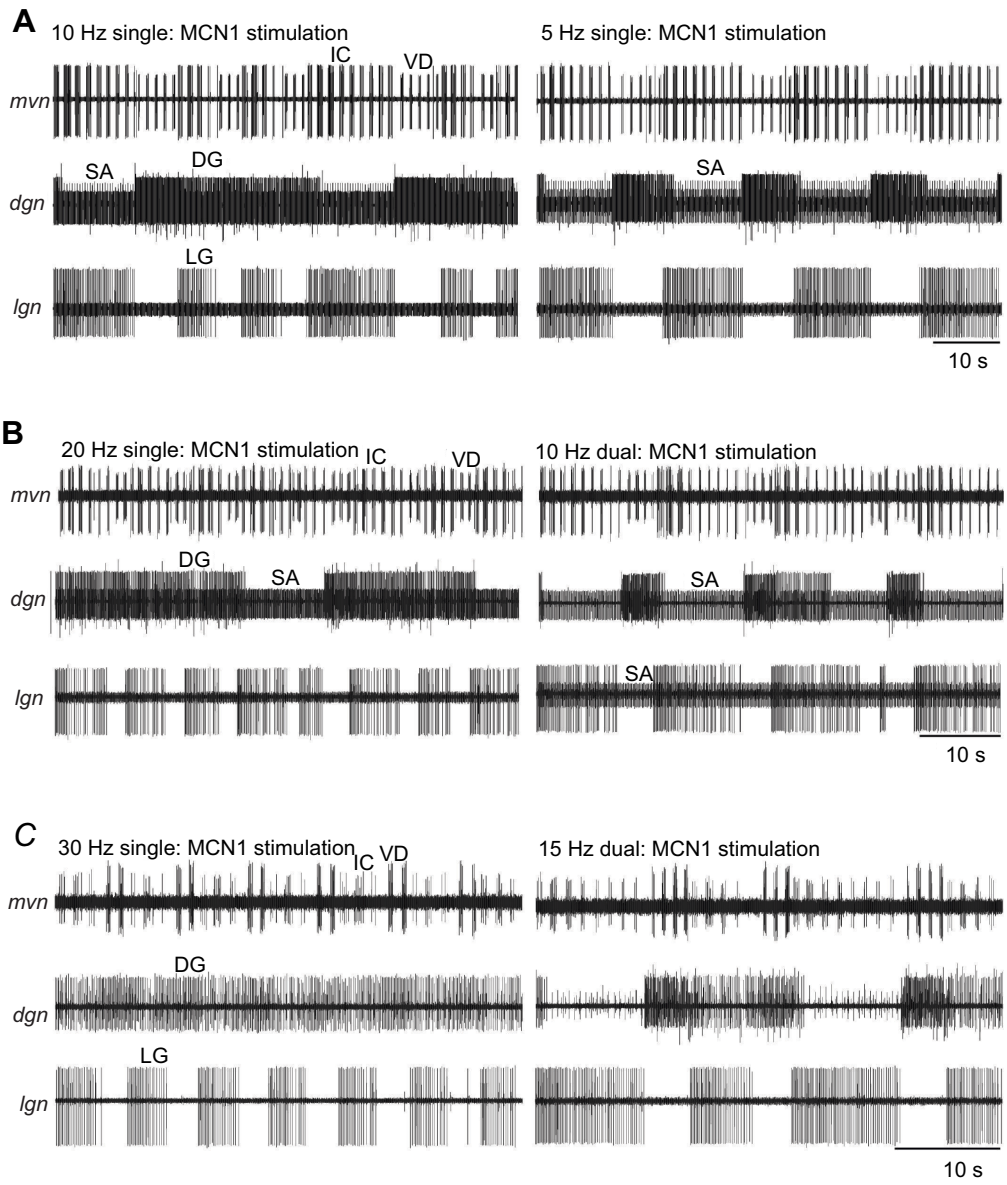

Fig. 4. Example recordings of matched pairs of dual and single MCN1-driven gastric mill rhythms on an expanded time scale. Note that unlike the poorly coordinated bursting between LG and DG, particularly during the single MCN1 stimulations, IC and VD neuron activity (*mvn*) consistently tracked LG activity. Each matched pair was recorded in the same experiment, but the different pairs come from different experiments. Matched MCN1 stimulations are compared at: (A) 5 Hz dual versus 10 Hz single; (B) 10 Hz dual versus 20 Hz single; (C) 15 Hz dual versus 30 Hz single. Filtered: *mvn*, all recordings; *dgn*, 10 Hz dual, 15 Hz dual, 30 Hz single. SA, stimulation artifact.

than during their matched single stimulations (10 Hz dual versus 20 Hz single: N=5, P=0.027; 15 Hz dual versus 30 Hz single: N=4, P=0.037, paired t-test). The larger DG firing rate reduction during protraction when both MCN1s were co-stimulated occurred despite the fact that the retraction phase firing rate of DG was equivalent during the matched dual and single stimulations (10 Hz dual, 12.5±0.6 Hz, N=5; 20 Hz single, 12.0±0.5 Hz, N=8, P=0.83; 15 Hz dual, 14.8±0.8 Hz, N=4; 30 Hz single, 13.4±0.3 Hz, N=8, P=0.35; unpaired t-test).

The failure of DG activity to terminate during protraction was particularly pronounced during 30 Hz single MCN1 stimulations. These stimulations rarely elicited LG–DG alternation in 50% or more gastric mill rhythm cycles (N=4/22, 18%), and only once (N=1/22, 4.5%) elicited alternation during 75% of the cycles (Fig. 3). Most of these 30 Hz single stimulations (15/22; 68%) exhibited no cycles in which DG was silenced during protraction. This latter type of response did not occur as frequently during the other stimulation protocols (5 Hz dual, 0%; 10 Hz single, 10%; 10 Hz dual, 18%; 20 Hz single, 45%; 15 Hz dual, 55%) (Fig. 3).

Distinct gastric mill rhythm parameters during matched dual and single MCN1 stimulations

There were also differences in several other gastric mill rhythm parameters between the matched dual and single MCN1 stimulations. For example, there was a longer gastric mill cycle period during the 5 Hz dual MCN1 stimulations than the 10 Hz single stimulations (N=14, P<0.001, one-way RM-ANOVA, Holm–Šidák *post hoc* test) (Figs 4A and 5A). Despite the rhythm being slower during the dual 5 Hz stimulation, there was no difference in protraction duration between the dual and single stimulations (N=13, P=0.14, RM-ANOVA) (Fig. 5B). Instead, the longer cycle period resulted from an increased retraction duration (N=14, P<0.001, RM-ANOVA on ranks, *post hoc* Tukey's test) (Fig. 5C). This selective prolongation of retraction during the dual 5 Hz MCN1 stimulations decreased the LG neuron duty cycle relative to the matched single stimulations (N=14, P<0.01; RM-ANOVA, Holm–Šidák *post hoc* t-test) (Fig. 5D). The effects of 10 Hz_L and 10 Hz_R single MCN1 stimulations were indistinguishable for this and all other examined parameters (N=14, P>0.05) (Fig. 5).

Journal of Experimental Biology (2020) 223, jeb228114. doi:10.1242/jeb.228114

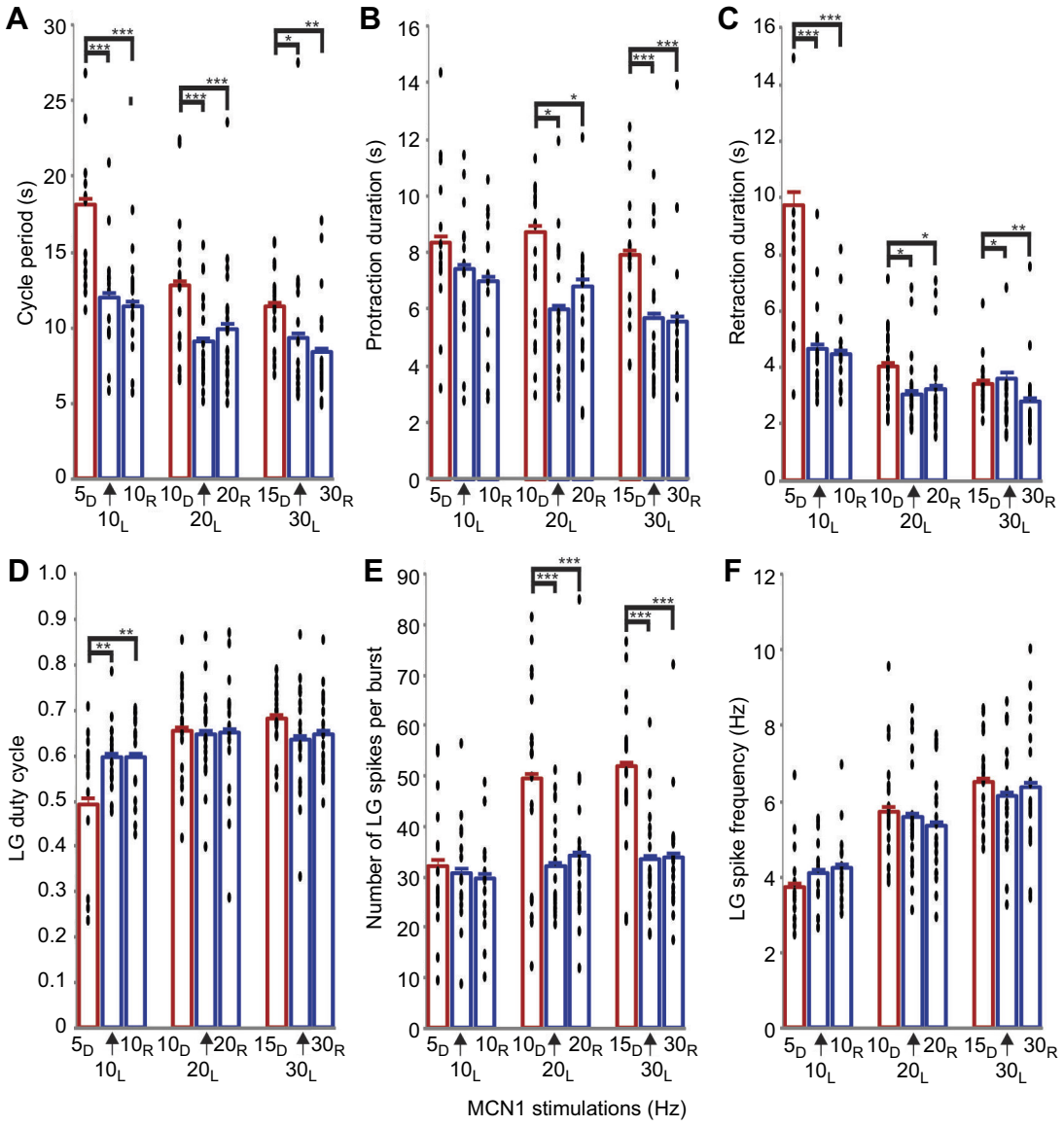

Fig. 5. Gastric mill rhythm parameters are distinct during matched dual and single MCN1 stimulations. Bar graphs display the mean gastric mill rhythm values during three sets of firing rate- and pattern-matched MCN1 stimulation protocols for (A) cycle period (outlier: 5 Hz dual, 33.8 s), (B) protraction duration (outliers: 10 Hz dual, 19.8 s, 17.4 s; 20 Hz_R, 22.1 s), (C) retraction duration (outlier: 5 Hz dual, 26.2 s, 19.4 s; 30 Hz_L, 18.5 s), (D) LG duty cycle, (E) number of LG spikes per burst and (F) LG intraburst firing rate. The mean values for each experiment are shown (filled ovals), excluding outliers which were omitted to optimize the *y*-axis dimensions. **P*<0.05, ***P*<0.01, ****P*<0.001; see Results for *N*-values and statistical tests.

At the higher MCN1 stimulation frequency sets (10 Hz dual versus 20 Hz single, *N*=19; 15 Hz dual versus 30 Hz single, *N*=18), protraction and retraction were both prolonged, and thus so was cycle period, during the dual MCN1 stimulations (Fig. 5A–C). In contrast, there was no distinction in these parameters between the single $MCN1_L$ and $MCN1_R$ stimulations at the same stimulation rate (Fig. 5A–C). The parallel increases in protraction and retraction duration during the higher dual stimulation rates resulted in there being no difference in the LG duty cycle between these conditions and their matched set of single MCN1 stimulations (Fig. 5C).

We also determined whether the LG neuron burst characteristics were differentially influenced by matched dual and single MCN1 stimulation. With respect to the number of LG spikes per burst, there was no difference at the lowest matched MCN1 stimulation rate (*N*=14, *P*=0.81, RM-ANOVA on ranks) (Fig. 5E). In contrast, during both of the higher matched stimulation rates, the dual stimulations consistently elicited more LG spikes per burst than their matched single MCN1 stimulations (10 Hz dual versus 20 Hz single: *P*<0.001, *N*=19; 15 Hz dual versus 30 Hz single: *P*<0.001, *N*=18; RM-ANOVA, Holm–Šidák *post hoc* test) (Fig. 5E). There was no change in the LG intraburst firing rate within any of the three sets of stimulation conditions (Fig. 5F). Instead, the increased LG spike numbers reflected the prolonged LG burst duration (Fig. 5B).

Because both MCN1s are co-activated by all identified input pathways, we also compared the gastric mill rhythms when both MCN1s were co-stimulated (10 Hz each) versus single MCN1 stimulation at the same frequency (*N*=13) (Fig. 6A,B). These stimulation conditions again elicited differences in some gastric mill rhythm parameters (Fig. 6B). For example, dual MCN1 stimulation (10 Hz each) elicited gastric mill rhythms exhibiting a longer cycle period (*P*=0.006) due to a prolonged protraction phase (*P*<0.001), with an increased LG duty cycle (*P*=0.003) containing more LG

Journal of Experimental Biology (2020) 223, jeb228114. doi:10.1242/jeb.228114

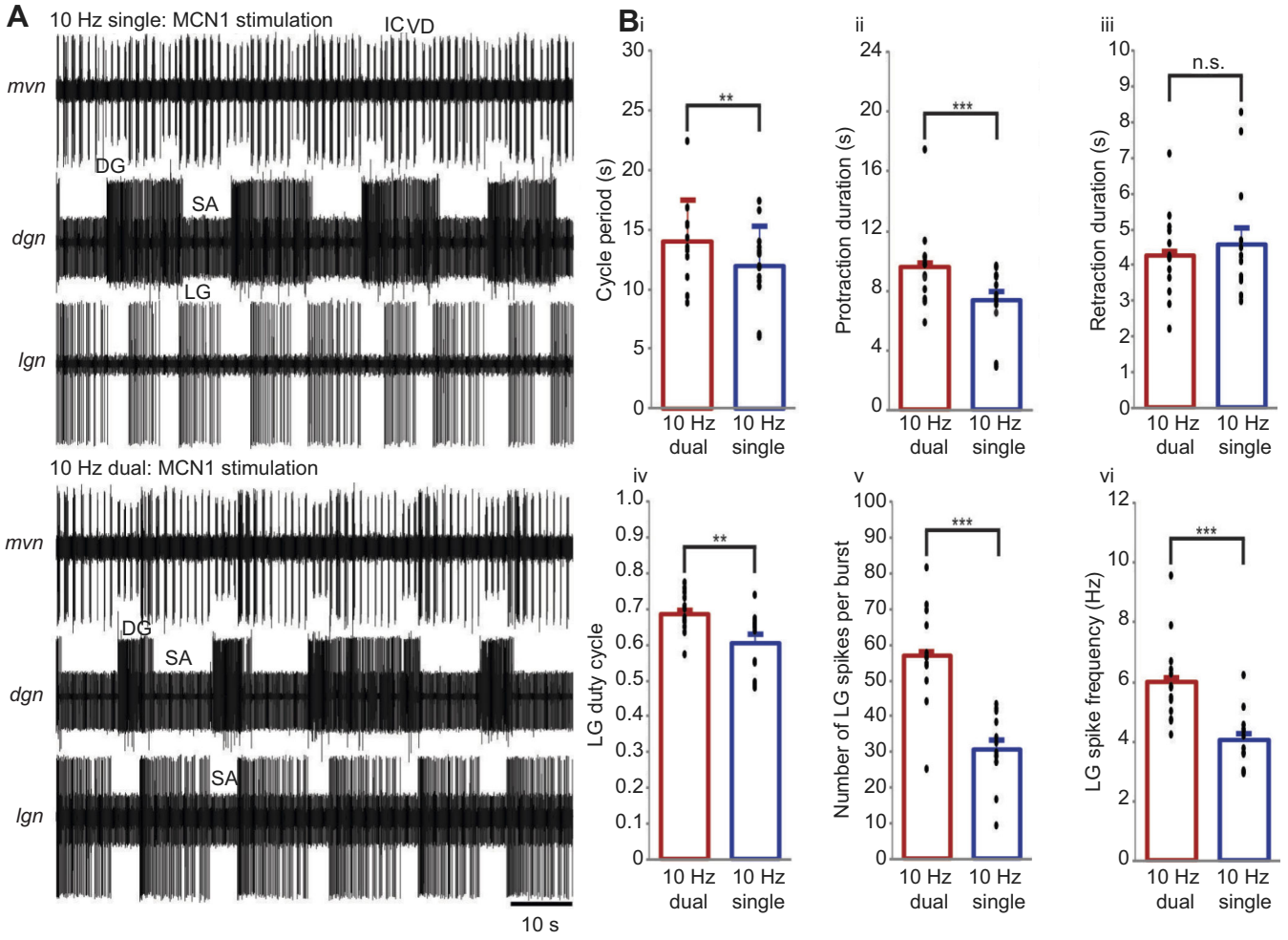

Fig. 6. Dual MCN1 stimulation, at 10 Hz each, drives a protraction-prolonged gastric mill rhythm with a higher LG neuron intraburst firing frequency relative to single MCN1 stimulation at 10 Hz. (A) Example gastric mill rhythms driven by dual (10 Hz each) and single MCN1 stimulations at 10 Hz. Filtered: 10 Hz single, *mvn*; 10 Hz dual, *mvn*, *dgn*. (B) Bar graphs compare the mean value for different gastric mill rhythm parameters during dual (10 Hz each) and single MCN1 stimulations (10 Hz; N=13). Filled ovals represent the mean values from each experiment. IC, inferior cardiac (neuron); SA, stimulation artifact; VD, ventricular dilator (neuron). (Bi) Cycle period: **P=0.006; (Bii) protraction duration: ***P<0.001; (Biii) retraction duration: $^{n.s.}P$=0.455; (Biv) LG duty cycle: **P=0.003; (Bv) number of LG spikes per burst: ***P<0.001; (Bvi) LG intraburst firing frequency: ***P<0.001. Bi,ii,iii,vi: Wilcoxon signed rank test; Biv,v: paired t-test. n.s., not significant.

spikes per burst (P<0.001) generated at a higher firing rate (P<0.001) than during single MCN1 stimulation at 10 Hz (Fig. 6B). There was no difference in the retraction phase duration (P=0.455).

In addition to differences in the mean value of some gastric mill rhythm parameters between matched dual and single MCN1 stimulation frequencies, we assessed parameter variability across experiments in relation to the mean using the coefficient of variation (CV). Statistically significant differences occurred primarily during the 5 Hz dual versus 10 Hz single stimulations. For example, the CV across experiments for cycle period was higher for the 10 Hz single MCN1 stimulations (dual MCN1 versus: $MCN1_L$, P=0.028; $MCN1_R$, P=0.031; RM-ANOVA, Holm–Šidák *post hoc* test; N=14) (Fig. 7A). Some of the studied parameters whose mean values were not different nevertheless exhibited differences in the CV, as was the case for the protraction duration and number of LG spikes per burst (Figs 5 and 7). For example, the protraction duration CV during the single 10 Hz stimulations for $MCN1_L$ was 0.27±0.01 s, while it was 0.17±0.01 s for the dual 5 Hz stimulation (N=14; P=0.045, RM-ANOVA, Holm–Šidák *post hoc* test). However, despite the 10 Hz stimulation of $MCN1_R$ having the same protraction duration CV as $MCN1_L$ (0.27±0.01), this value was not different from that of the matched 5 Hz dual stimulations (P=0.062, RM-ANOVA, Holm–Šidák *post hoc* test). With respect to the number of LG spikes per burst, single MCN1 stimulations at 10 Hz produced a higher CV across experiments than the dual 5 Hz stimulation (dual MCN1 versus: $MCN1_L$, P=0.03; $MCN1_R$, P=0.042; RM-ANOVA, Holm–Šidák *post hoc* test; N=14). In contrast, the CV for retraction duration, LG duty cycle and LG firing frequency was comparable for the matched dual (5 Hz each) and single (10 Hz) MCN1 stimulations (Fig. 7C,D,F). Few parameters exhibited CV differences between the higher frequency-matched MCN1 stimulations, and in no cases did both single stimulations differ from the matched dual stimulation (Fig. 7).

The LG neuron bursts weaken but do not eliminate $MCN1_{STG}$ synaptic actions

The fact that DG neuron activity was not always limited to the retraction phase in these experiments, but exhibited a reduced firing rate when active during protraction (Figs 2–4), suggested

Journal of Experimental Biology (2020) 223, jeb228114. doi:10.1242/jeb.228114

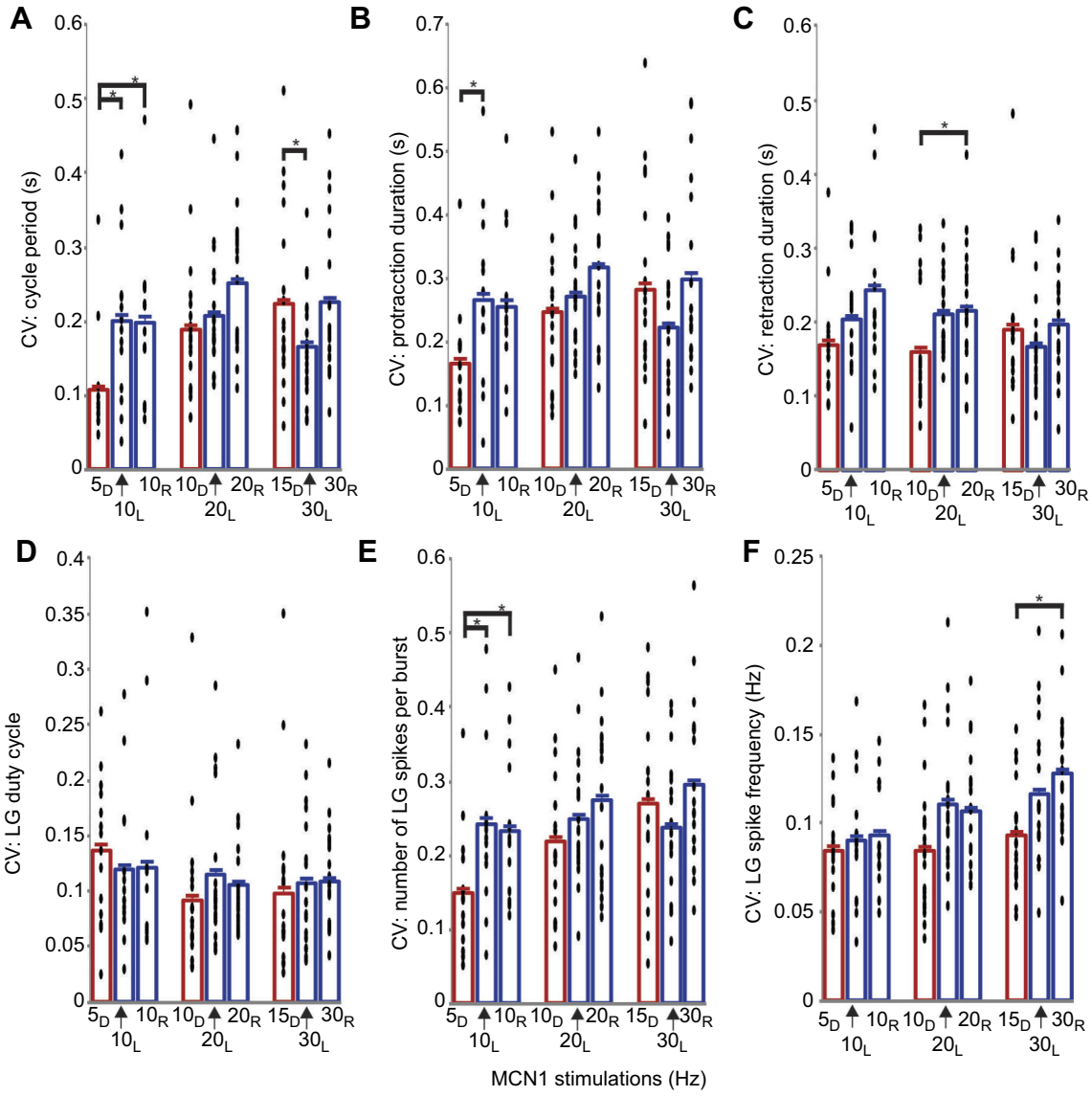

Fig. 7. The inter-experiment coefficient of variation for some gastric mill rhythm parameters is distinct between matched dual and single MCN1 stimulations. Bar graphs display the mean gastric mill rhythm coefficient of variation (CV) values during three sets of firing rate- and pattern-matched MCN1 stimulation protocols for (A) cycle period, (B) protraction duration, (C) retraction duration, (D) LG duty cycle, (E) number of LG spikes per burst and (F) LG intraburst firing rate. The mean values for each experiment are shown as filled ovals. *P<0.05, RM-ANOVA plus Holm–Šidák *post hoc* test for all comparisons except cycle period for 15 Hz dual versus 30 Hz single (RM-ANOVA on ranks plus Tukey's *t*-test). See Results for *N*-values and statistical tests.

that the LG firing frequency during these rhythms weakened but did not eliminate $MCN1_{STG}$ transmitter release. We used matched dual (10 Hz) and single (20 Hz) MCN1 stimulations to test this hypothesis by comparing the influence of natural and strengthened LG bursts on two targets that it only affects via its inhibition of $MCN1_{STG}$, including (a) DG neuron activity and (b) the pyloric cycle period. The pyloric cycle period is a useful assay because MCN1 directly excites the pyloric rhythm, reducing the pyloric cycle period, whereas LG activity only influences this rhythm (i.e. increases the pyloric cycle period) via its inhibition of $MCN1_{STG}$ (Fig. 1C) (Bartos and Nusbaum, 1997).

When LG neuron activity was strengthened during matched dual (10 Hz) and single (20 Hz) MCN1 stimulations, its increased firing rate was not different across protocols (20 Hz_L: 13.9±0.4 Hz; 20 Hz_R: 13.4±0.4 Hz; 10 Hz_{both}: 13.1±0.6 Hz; N=5 experiments, 10 LG depolarizations per condition; P=0.111, RM-ANOVA). These increased firing rates were consistently higher than during the control LG bursts (P<0.001 for each protocol, RM-ANOVA, Holm–Šidák *post hoc* test), which ranged from 4.5 to 6.0 Hz.

For gastric mill rhythm cycles where DG neuron activity extended through the LG burst, enhanced LG activity eliminated this prolonged DG activity in 9/20 cycles during 20 Hz single MCN1 stimulations (45%; N=5 experiments, two LG current injections per MCN1 stimulation). In the remaining 11 cycles, the DG firing rate was weakened but not terminated. This extended DG activity was more consistently eliminated during the dual 10 Hz MCN1 stimulations (9/10 cycles 90%; n=5 experiments, two LG current injections per MCN1 stimulation; P=0.024, Fisher's exact test), suggesting that LG more effectively regulates MCN1 activity when MCN1 fires at a lower rate.

Journal of Experimental Biology (2020) 223, jeb228114. doi:10.1242/jeb.228114

We evaluated the impact of an increased LG firing frequency on the pyloric cycle period by first normalizing the pyloric cycle period during strengthened LG firing to that during the preceding, control LG burst ('LG depolarization ratio'; see Materials and Methods). We then compared this normalized value with a control value obtained by dividing the pyloric cycle period during the same, preceding control LG burst by the cycle period during the control LG burst two prior to the depolarized LG burst ('control ratio'). The control pyloric cycle period ratios were comparable across all MCN1 stimulation protocols (N=10 stimulations per protocol, P=0.407, repeated measures ANOVA on ranks).

During all three sets of MCN1 stimulation, the LG depolarization ratio was larger than the control ratio [20 Hz_L: LG depolarization ratio, 1.11±0.03; control ratio, 1.00±0.03, P=0.004; 20 Hz_R: LG depolarization ratio, 1.18±0.06; control ratio, 0.99±0.01, P=0.004; 10 Hz_{Both}: LG depolarization ratio, 1.07±0.01; control ratio, 0.99 ±0.01, P=0.001; N=5, signed rank test (20 $Hz_{L,R}$), paired t-test (10 Hz_{both})] (Fig. 8). The increased ratios that occurred during the LG current injections indicated that the pyloric cycle period at these times was prolonged relative to that during the control LG bursts. Consistent with the limited LG–DG alternation reported above (Figs 2–4), and the impact of an increased LG firing rate on the timing of DG neuron bursts, these pyloric rhythm results suggested that the strengthened LG bursts more strongly inhibit $MCN1_{STG}$ transmitter release.

Long-lasting activation of MCN1 mimics the effects of extracellular MCN1 stimulation

We used *ion* stimulation to selectively drive MCN1 despite the presence of another CoG neuron (MCN5) that projects to the STG through the *ion* because MCN1 has a lower stimulation threshold (see Materials and Methods). We nevertheless considered the possibility that some MCN5 stimulation contributed to our results by comparing the influence of *ion* stimulation with that resulting from activating MCN1 by stimulating the *dpon*, after bisecting the *son* medial to the *dpon* (see Materials and Methods) (Fig. 1A).

The MCN1 firing rate resulting from *dpon* stimulation in different experiments ranged from 9.5 to 26 Hz. To match the *ion* and *dpon* activation of MCN1 in each experiment, we first triggered a VCN activation of MCN1 and recorded the resulting gastric mill rhythm. In parallel, we determined the VCN-triggered MCN1 firing rate and used that same rate to subsequently stimulate the *ion*. We then followed each *ion* stimulation with a second *dpon* stimulation. Little or no MCN5 activity was evident in the *ion* recordings during the VCN-triggered gastric mill rhythms. We assayed the gastric mill rhythm response by analysing the same gastric mill rhythm parameters as above (Fig. 5) and determining the gastric mill rhythm-timed activity of the DG neuron.

The gastric mill microcircuit response to *dpon* and *ion* stimulation was comparable for five of the six analysed parameters, including cycle period, protraction and retraction duration, number of LG spikes per burst, and the LG duty cycle (N=5) (Fig. 9). The only analysed parameter with distinct values was the LG neuron firing frequency (*dpon* stimulation 1: 6.6±1.1 Hz; *ion* stimulation: 5.9±0.9 Hz; *dpon* stimulation 2: 6.5±1.0 Hz; N=5; *dpon*1 versus *ion*: P=0.03; *dpon*2 versus *ion*: P=0.04; *dpon*1 versus *dpon*2: P=0.67, RM-ANOVA, Holm–Šidák *post hoc* test) (Fig. 9F). Similarly, the matched MCN1 firing rates from *dpon* and *ion* stimulations resulted in comparable DG neuron activity patterns. In none of these experiments was DG activity limited to the retraction phase, nor were there any gastric mill rhythms in which the LG and DG bursts alternated in at least 50% of the cycles (N=5).

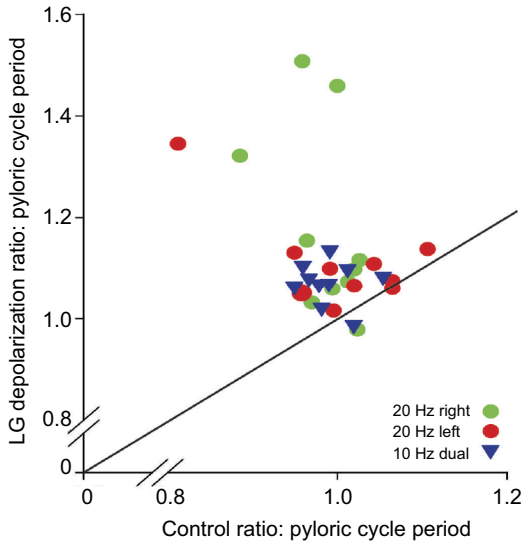

Fig. 8. The pyloric cycle period is prolonged by increasing the intraburst LG firing frequency. Scatter plot showing the ratio of the pyloric cycle period during an enhanced LG burst to that of the preceding LG burst (LG depolarization ratio) relative to its control ratio, during gastric mill rhythms driven by single (20 Hz) or dual (10 Hz) MCN1 stimulation (N=10: five experiments, two LG depolarizations per experiment for each single and dual MCN1 stimulation). Diagonal line slope=1.

DISCUSSION

In this paper we determined that firing rate- and pattern-matched dual and single stimulation of the paired projection neuron MCN1 does not elicit equivalent gastric mill motor patterns. These different outcomes appear due, at least partly, to a mismatch in the firing rate of MCN1 and the gastric mill microcircuit neuron LG, which regulates MCN1 transmission in the STG via presynaptic inhibition (Fig. 1D) (Coleman and Nusbaum, 1994; Coleman et al., 1995). Specifically, the dual MCN1 stimulations more consistently elicited completely coordinated gastric mill cycles. This coordination distinction was particularly pronounced at the lowest MCN1 stimulation frequency comparison, during which the dual stimulations also exhibited lower variability in several parameters across experiments. This outcome suggests that acute loss of one MCN1 would compromise behavioral performance to the extent that effective chewing involves coordinated rhythmic protraction and retraction of the teeth (Heinzel et al., 1993; Diehl et al., 2013). Functional recovery after such a loss might be facilitated, however, by long-term compensatory mechanisms that are known to occur in some motor systems (Büschges et al., 1992; Sánchez et al., 2000; Sakurai and Katz, 2009; Fink and Cafferty, 2016; Sakurai et al., 2016; Brown and Martinez, 2018; Puhl et al., 2018).

Insofar as most gastric mill microcircuit neurons are also the motor neurons for the system, the other rhythm parameter differences that we identified suggest that differences would also occur in the response dynamics of at least some gastric mill muscles, producing changes in the timing and/or strength of teeth movements (Stein et al., 2006; Diehl et al., 2013). Whether these latter changes would compromise chewing behavior, however, remains to be determined. In all comparisons, there were no differences between the matched single stimulations ($MCN1_L$ versus $MCN1_R$), which is consistent with previous evidence suggesting that the two MCN1s are functionally equivalent. There do not appear to be other studies

Journal of Experimental Biology (2020) 223, jeb228114. doi:10.1242/jeb.228114

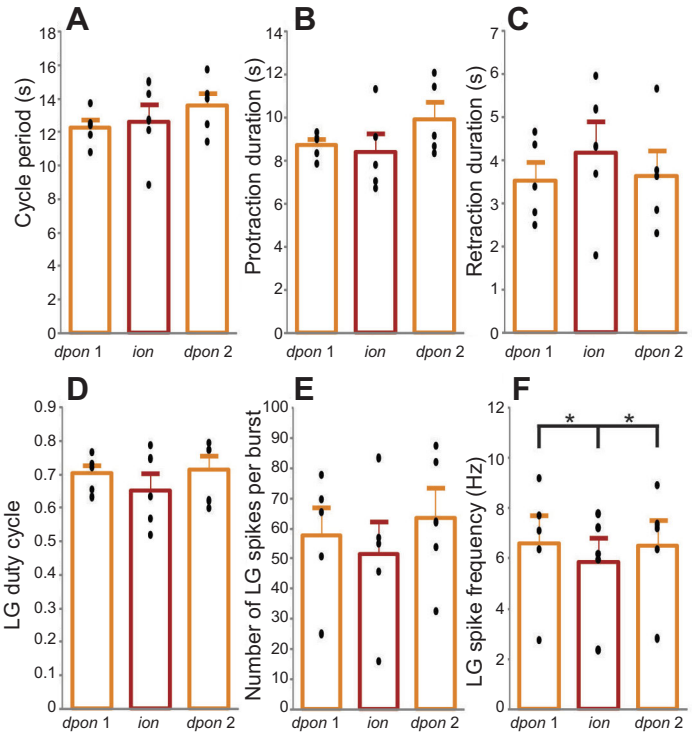

Fig. 9. VCN stimulation with the *son*s bisected elicits a MCN1–gastric mill rhythm comparable to that resulting from *ion* stimulation using the same MCN1 firing rate. Bar graphs display the mean gastric mill rhythm values triggered by VCN stimulation, before (*dpon*1) and after (*dpon*2) MCN1 (*ion*) stimulation for (A) cycle period, (B) protraction duration, (C) retraction duration, (D) LG duty cycle, (E) number of LG spikes per burst and (F) LG intraburst firing rate. Mean values for each experiment are shown as filled circles (N=5). *P=0.04, RM-ANOVA plus Holm–Šidák *post hoc* test.

that performed such a comparison on different copies of a projection neuron within the same preparations.

The role(s) of presynaptic regulation of projection- and sensory neuron inputs to microcircuits remains under-explored despite its established presence, often at multiple locations, in several neural systems (Nusbaum, 1994; Sillar and Simmers, 1994; Krieger et al., 1996; Cochilla and Alford, 1999; Westberg et al., 2000; Takahashi and Alford, 2002; Evans et al., 2003; Hurwitz et al., 2005; Barrière et al., 2008; Blitz and Nusbaum, 2008, 2012; Jing et al., 2011; Wang, 2012; McGann, 2013; Sirois et al., 2013; Blitz et al., 2019). For the MCN1–gastric mill rhythm, the pivotal role of LG neuron presynaptic inhibition of $MCN1_{STG}$ suggests that this circuit design favors dual MCN1 activity over firing rate-matched single MCN1 activity. This suggestion is consistent with the greater effectiveness of this presynaptic action during the dual MCN1 stimulations, where each MCN1 fired at half the rate of the matched single MCN1 stimulations, and by our finding that the LG firing rate was equivalent within each matched set of MCN1 stimulations. This outcome resulted from the LG synaptic action reducing but not eliminating MCN1 transmitter release in these experiments, insofar as increasing the LG intraburst firing rate during both dual and single MCN1 stimulation more consistently limited DG neuron activity to the retraction phase, and further weakened the pyloric rhythm. LG only regulates these two events via its inhibitory action on $MCN1_{STG}$ (Coleman and Nusbaum, 1994; Bartos and Nusbaum, 1997). This is the first indication in the biological system that the gastric mill rhythm-timed LG bursts reduce but do not eliminate $MCN1_{STG}$ transmitter release, although a previous computational model did support this possibility (DeLong et al., 2009b).

The prolonged gastric mill cycle period during the dual MCN1 stimulations resulted from selectively prolonged retraction during dual 5 Hz MCN1 stimulation, whereas both phases were prolonged during the dual 10 Hz and 15 Hz MCN1 stimulations. This distinction suggests that different cellular/synaptic mechanisms underlie cycle period regulation during different MCN1 firing rates. Selectively prolonged retraction occurs when the accumulation rate of the voltage-dependent inward current I_{MI} in LG is reduced at times when there is little or no change in the strength of Int1-mediated inhibition (Beenhakker et al., 2005; DeLong et al., 2009a,b). During each retraction phase, MCN1-released CabTRP Ia peptide re-initiates a slow build-up of I_{MI} in LG, because the previous build-up had decayed during protraction (Fig. 1D). In the present study, this prolonged retraction phase may have resulted from a relatively low release rate of CabTRP Ia peptide when each MCN1 is firing at 5 Hz, a firing rate that commonly generates a near-threshold level of neuropeptide release (Vilim et al., 1996, 2000; Liu et al., 2011; Ding et al., 2019). MCN1-released CabTRP Ia peptide activates I_{MI} in LG, and 5 Hz is the approximate threshold firing frequency for the MCN1-driven gastric mill rhythm (Wood et al., 2000; Kirby and Nusbaum, 2007; DeLong et al., 2009b). Selectively prolonged retraction may also result from I_{MI} declining to a lower level at the end of each LG burst during the 5 Hz dual MCN1 stimulations relative to the matched 10 Hz single stimulations, owing to LG more strongly inhibiting $MCN1_{STG}$ transmitter release at the lower MCN1 firing rate. After a stronger LG inhibition of $MCN1_{STG}$, more time would be needed for sufficient I_{MI} to build up and trigger the next LG burst (DeLong et al., 2009b).

How the dual 10 Hz and 15 Hz MCN1 stimulations prolonged both gastric mill rhythm phases relative to their matched single stimulations is less clear. However, MCN1 activity does prolong both phases when Int1 inhibition of LG is strengthened to a greater degree than the parallel rate of I_{MI} build-up (Beenhakker et al., 2005). At the higher MCN1 stimulation frequencies the dual stimulations may alter the balance of CabTRP Ia and GABA release, relative to their matched single stimulations, such that the MCN1 GABAergic excitation of Int1 becomes relatively more strengthened than the peptidergic excitation of LG. Neuropeptide and small molecule transmitter release can have different Ca^{2+} and/or firing rate dependencies (Whim and Lloyd, 1989; Peng and Zucker, 1993; Liu et al., 2011; Nusbaum et al., 2017). Also, as above, the more

effective LG inhibition of $MCN1_{STG}$ during the dual stimulations would be likely to more completely reduce I_{MI} amplitude at the end of each LG burst, contributing to a longer duration for I_{MI} build-up during each subsequent retraction phase.

In contrast to these experiments, where optimal generation of a fully coordinated gastric mill rhythm resulted from dual MCN1 stimulation at 5 Hz, the MCN1 firing rate is often considerably higher (25–30 Hz) during fully coordinated gastric mill rhythms triggered by the VCN or POC neurons in the complete STNS (Beenhakker and Nusbaum, 2004; Blitz and Nusbaum, 2012). However, the VCN- and POC-triggered gastric mill rhythms are driven by co-activating MCN1 and CPN2, another CoG projection neuron. Also, during these latter rhythms the firing pattern of both projection neurons is not tonic but is rhythmically coordinated with the gastric mill and pyloric rhythms, due to synaptic input from the gastric mill and pyloric microcircuit interneurons Int1 and AB. Microcircuit output-linked activity patterns in projection neurons that drive rhythmic motor patterns are common across systems (Weeks and Kristan, 1978; Rosen et al., 1991; Norris et al., 1994, 1996; Puhl et al., 2012; Grillner and El Manira, 2020). It remains to be determined whether some or all of these distinctions, as well as the rhythmic sensory feedback that would be present *in vivo*, compensate for the degraded coordinated activity that occurred under many of our experimental conditions in the isolated STG. Although rhythmic sensory feedback is not necessary for core rhythm generation in most motor systems, such feedback commonly sculpts the final motor pattern *in vivo* (Wolf and Pearson, 1988; Hooper et al., 1990; Büschges et al., 1992; Combes et al., 1999; Eisenhart et al., 2000; Marder and Bucher, 2001; Smarandache and Stein, 2007; Hedrich et al., 2009; Büschges et al., 2011; Akay et al., 2014). Additionally, regarding this latter issue, DG neuron-mediated muscle contraction activates the muscle stretch-sensitive neuron GPR (Katz et al., 1989). GPR activity, in turn, excites MCN1 and CPN2 in both CoGs, influences the gastric mill rhythm generator neurons in the STG, and can entrain the gastric mill rhythm (Blitz et al., 2004; Beenhakker et al., 2005). Thus, this sensory feedback pathway may normally provide a correction signal that maintains MCN1-driven gastric mill rhythm coordination *in vivo*.

The superior coordination of gastric mill rhythms driven by dual MCN1 stimulation provides a reasonable explanation for why all identified inputs to MCN1 influence both copies, despite their presence in separate ganglia (Beenhakker et al., 2004, 2005; Blitz et al., 2004, 2008; Christie et al., 2004; Hedrich et al., 2009; Blitz and Nusbaum, 2012; White et al., 2017). This system design also provides a cautionary note for efforts focused on enabling recovery of function after partial loss of pathways that drive behavior. Increasing the firing rate of the remaining copies in a compromised pathway might be expected to compensate for partial loss of some copy members, but this is not the only possible outcome. For example, as noted above, neurons often exhibit firing rate-dependent changes in neurotransmitter release that can alter the balance of their ionotropic and metabotropic actions, leading to qualitative changes in microcircuit output. Additionally, insofar as neurotransmitter release for many neurons is also regulated locally at axon terminals, the balance between the projection neuron firing rate and that of the regulating presynaptic neuron can be pivotal to maintaining a coordinated motor pattern, as is the case for MCN1. In conclusion, the gastric mill microcircuit is more effectively driven by co-activating the paired projection neuron MCN1 than by its firing rate- and pattern matched single stimulation, at least in the isolated nervous system.

Acknowledgements
We thank Mr Logan Fickling for helpful feedback on earlier versions of the manuscript and for assistance in preparing Fig. 3.

Competing interests
The authors declare no competing or financial interests.

Author contributions
Conceptualization: G.F.C., A.P.C., M.P.N.; Methodology: G.F.C., A.P.C., M.P.N.; Formal analysis: G.F.C., A.P.C.; Investigation: G.F.C., A.P.C.; Resources: M.P.N.; Data curation: G.F.C., A.P.C.; Writing - original draft: M.P.N.; Writing - review & editing: G.F.C., A.P.C., M.P.N.; Visualization: A.P.C.; Supervision: M.P.N.; Project administration: M.P.N.; Funding acquisition: M.P.N.

Funding
This work was supported by the National Institute of Neurological Disorders and Stroke (R01-NS029436 to M.P.N.). Deposited in PMC for release after 12 months.

References

Akay, T., Tourtellotte, W. G., Arber, S. and Jessell, T. M. (2014). Degradation of mouse locomotor pattern in the absence of proprioceptive sensory feedback. *Proc. Natl. Acad. Sci. USA* **111**, 16877-16882. doi:10.1073/pnas.1419045111

Arrigoni, E. and Saper, C. B. (2014). What optogenetic stimulation is telling us (and failing to tell us) about fast neurotransmitters and neuromodulators in brain circuits for wake-sleep regulation. *Curr. Opin. Neurobiol.* **29**, 165-171. doi:10.1016/j.conb.2014.07.016

Barrière, G., Simmers, J. and Combes, D. (2008). Multiple mechanisms for integrating proprioceptive inputs that converge on the same motor pattern-generating network. *J. Neurosci.* **28**, 8810-8820. doi:10.1523/JNEUROSCI.2095-08.2008

Bartos, M. and Nusbaum, M. P. (1997). Inter-circuit control of motor pattern modulation by presynaptic inhibition. *J. Neurosci.* **17**, 2247-2256. doi:10.1523/JNEUROSCI.17-07-02247.1997

Bartos, M., Manor, Y., Nadim, F., Marder, E. and Nusbaum, M. P. (1999). Coordination of fast and slow rhythmic neuronal circuits. *J. Neurosci.* **19**, 6650-6660. doi:10.1523/JNEUROSCI.19-15-06650.1999

Beenhakker, M. P. and Nusbaum, M. P. (2004). Mechanosensory activation of a motor circuit by coactivation of two projection neurons. *J. Neurosci.* **24**, 6741-6750. doi:10.1523/JNEUROSCI.1682-04.2004

Beenhakker, M. P., Blitz, D. M. and Nusbaum, M. P. (2004). Long-lasting activation of rhythmic neuronal activity by a novel mechanosensory system in the crustacean stomatogastric nervous system. *J. Neurophysiol.* **91**, 78-91. doi:10.1152/jn.00741.2003

Beenhakker, M. P., DeLong, N. D., Saideman, S. R., Nadim, F. and Nusbaum, M. P. (2005). Proprioceptor regulation of motor circuit activity by presynaptic inhibition of a modulatory projection neuron. *J. Neurosci.* **25**, 8794-8806. doi:10.1523/JNEUROSCI.2663-05.2005

Betley, J. N., Cao, Z. F., Ritola, K. D. and Sternson, S. M. (2013). Parallel, redundant circuit organization for homeostatic control of feeding behavior. *Cell* **155**, 1337-1350. doi:10.1016/j.cell.2013.11.002

Bidaye, S. S., Machacek, C., Wu, Y. and Dickson, B. J. (2014). Neuronal control of *Drosophila* walking direction. *Science* **344**, 97-101. doi:10.1126/science.1249964

Blitz, D. M. and Nusbaum, M. P. (2008). State-dependent presynaptic inhibition regulates central pattern generator feedback to descending inputs. *J. Neurosci.* **28**, 9564-9574. doi:10.1523/JNEUROSCI.3011-08.2008

Blitz, D. M. and Nusbaum, M. P. (2012). Modulation of circuit feedback specifies motor circuit output. *J. Neurosci.* **32**, 9182-9193. doi:10.1523/JNEUROSCI.1461-12.2012

Blitz, D. M., Beenhakker, M. P. and Nusbaum, M. P. (2004). Different sensory systems share projection neurons but elicit distinct motor patterns. *J. Neurosci.* **24**, 11381-11390. doi:10.1523/JNEUROSCI.3219-04.2004

Blitz, D. M., Christie, A. E., Coleman, M. J., Norris, B. J., Marder, E. and Nusbaum, M. P. (1999). Different proctolin neurons elicit distinct motor patterns from a multifunctional neuronal network. *J. Neurosci.* **19**, 5449-5463. doi:10.1523/JNEUROSCI.19-13-05449.1999

Blitz, D. M., Christie, A. E., Cook, A. P., Dickinson, P. S. and Nusbaum, M. P. (2019). Similarities and differences in circuit responses to applied Gly1-SIFamide and peptidergic (Gly1-SIFamide) neuron stimulation. *J. Neurophysiol.* **121**, 950-972. doi:10.1152/jn.00567.2018

Blitz, D. M., White, R. S., Saideman, S. R., Cook, A., Christie, A. E., Nadim, F. and Nusbaum, M. P. (2008). A newly identified extrinsic input triggers a distinct gastric mill rhythm via activation of modulatory projection neurons. *J. Exp. Biol.* **211**, 1000-1011. doi:10.1242/jeb.015222

Brodfuehrer, P. D. and Thorogood, M. S. E. (2001). Identified neurons and leech swimming behavior. *Prog. Neurobiol.* **63**, 371-381. doi:10.1016/S0301-0082(00)00048-4

Brown, A. R. and Martinez, M. (2018). Ipsilesional motor cortex plasticity participates in spontaneous hindlimb recovery after lateral hemisection of the

thoracic spinal cord in the rat. *J. Neurosci.* **38**, 9977-9988. doi:10.1523/JNEUROSCI.1062-18.2018
Büschges, A., Ramirez, J.-M. and Pearson, K. G. (1992). Reorganization of sensory regulation of locust flight after partial deafferentation. *J. Neurobiol.* **23**, 31-43. doi:10.1002/neu.480230105
Büschges, A., Scholz, H. and El Manira, A. (2011). New moves in motor control. *Curr. Biol.* **21**, R513-R524. doi:10.1016/j.cub.2011.05.029
Cazalis, M., Dayanithi, G. and Nordmann, J. J. (1985). The role of patterned burst and interburst interval on the excitation-coupling mechanism in the isolated rat neural lobe. *J. Physiol.* **369**, 45-60. doi:10.1113/jphysiol.1985.sp015887
Christie, A. E., Stein, W., Quinlan, J. E., Beenhakker, M. P., Marder, E. and Nusbaum, M. P. (2004). Actions of a histaminergic/peptidergic projection neuron on rhythmic motor patterns in the stomatogastric nervous system of the crab *Cancer borealis*. *J. Comp. Neurol* **469**, 153-169. doi:10.1002/cne.11003
Cochilla, A. J. and Alford, S. (1999). NMDA receptor-mediated control of presynaptic calcium and neurotransmitter release. *J. Neurosci.* **19**, 193-205. doi:10.1523/JNEUROSCI.19-01-00193.1999
Coleman, M. J. and Nusbaum, M. P. (1994). Functional consequences of compartmentalization of synaptic input. *J. Neurosci.* **14**, 6544-6552. doi:10.1523/JNEUROSCI.14-11-06544.1994
Coleman, M. J., Meyrand, P. and Nusbaum, M. P. (1995). Presynaptic inhibition mediates a switch between two modes of synaptic transmission. *Nature* **378**, 502-505. doi:10.1038/378502a0
Coleman, M. J., Nusbaum, M. P., Cournil, I. and Claiborne, B. J. (1992). Distribution of modulatory inputs to the stomatogastric ganglion of the crab, *Cancer borealis*. *J. Comp. Neurol.* **325**, 581-594. doi:10.1002/cne.903250410
Combes, D., Meyrand, P. and Simmers, J. (1999). Dynamic restructuring of a rhythmic motor program by a single mechanoreceptor neuron in lobster. *J. Neurosci.* **19**, 3620-3628. doi:10.1523/JNEUROSCI.19-09-03620.1999
Cregg, J. M., Leiras, R., Montalant, A., Wanken, P., Wickersham, I. R. and Kiehn, O. (2020). Brainstem neurons that command mammalian locomotor asymmetries. *Nat. Neurosci.* **23**, 730-740. doi:10.1038/s41593-020-0633-7
Daghfous, G., Green, W. W., Alford, S. T., Zielinski, B. S. and Dubuc, R. (2016). Sensory activation of command cells for locomotion and modulatory mechanisms: lessons from lampreys. *Front. Neural Circuits.* **10**, 18. doi:10.3389/fncir.2016.00018
Daur, N., Nadim, F. and Bucher, D. (2016). The complexity of small circuits: the stomatogastric nervous system. *Curr. Opin. Neurobiol.* **41**, 1-7. doi:10.1016/j.conb.2016.07.005
DeLong, N. D., Beenhakker, M. P. and Nusbaum, M. P. (2009a). Presynaptic inhibition selectively weakens peptidergic cotransmission in a small motor system. *J. Neurophysiol.* **102**, 3492-3504. doi:10.1152/jn.00833.2009
DeLong, N. D., Kirby, M. S., Blitz, D. M. and Nusbaum, M. P. (2009b). Parallel regulation of a modulator-activated current via distinct dynamics underlies comodulation of motor circuit output. *J. Neurosci.* **29**, 12355-12367. doi:10.1523/JNEUROSCI.3079-09.2009
Dickinson, P. S., Sreekrishnan, A., Kwiatkowski, M. A. and Christie, A. E. (2015). Distinct or shared actions of peptide family isoforms: I. Peptide-specific actions of pyrokinins in the lobster cardiac neuromuscular system. *J. Exp. Biol.* **218**, 2892-2904. doi:10.1242/jeb.124800
Diehl, F., White, R. S., Stein, W. and Nusbaum, M. P. (2013). Motor circuit-specific burst patterns drive different muscle and behavior patterns. *J. Neurosci.* **33**, 12013-12029. doi:10.1523/JNEUROSCI.1060-13.2013
Ding, K., Han, Y., Seid, T. W., Buser, C., Karigo, T., Zhang, S., Dickman, D. K. and Anderson, D. J. (2019). Imaging neuropeptide release at synapses with a genetically engineered reporter. *eLife* **8**, e46421. doi:10.7554/eLife.46421
Eisenhart, F. J., Cacciatore, T. W. and Kristan, W. B., Jr (2000). A central pattern generator underlies crawling in the medicinal leech. *J. Comp. Physiol. A* **186**, 631-643. doi:10.1007/s003590000117
Evans, C. G., Jing, J., Rosen, S. C. and Cropper, E. C. (2003). Regulation of spike initiation and propagation in an *Aplysia* sensory neuron: gating-in via central depolarization. *J. Neurosci.* **23**, 2920-2931. doi:10.1523/JNEUROSCI.23-07-02920.2003
Fink, K. L. and Cafferty, W. B. (2016). Reorganization of intact descending motor circuits to replace lost connections after injury. *Neurotherapeutics* **13**, 370-381. doi:10.1007/s13311-016-0422-x
Fino, E., Vandecasteele, M., Perez, S., Saudou, F. and Venance, L. (2018). Region-specific and state-dependent action of striatal GABAergic interneurons. *Nat. Commun.* **9**, 3339. doi:10.1038/s41467-018-05847-5
Flamm, R. E. and Harris-Warrick, R. M. (1986). Aminergic modulation in lobster stomatogastric ganglion. I. Effects on motor pattern and activity of neurons within the pyloric circuit. *J. Neurophysiol.* **55**, 847-865. doi:10.1152/jn.1986.55.5.847
Fort, T. J., García-Crescioni, K., Agricola, H.-J., Brezina, V. and Miller, M. W. (2007). Regulation of the crab heartbeat by crustacean cardioactive peptide (CCAP): central and peripheral actions. *J. Neurophysiol.* **97**, 3407-3420. doi:10.1152/jn.00939.2006
Frost, W. N. and Katz, P. S. (1996). Single neuron control over a complex motor program. *Proc. Natl. Acad. Sci. USA* **93**, 422-426. doi:10.1073/pnas.93.1.422
Golowasch, J. and Marder, E. (1992). Proctolin activates an inward current whose voltage dependence is modified by extracellular Ca^{2+}. *J. Neurosci.* **12**, 810-817. doi:10.1523/JNEUROSCI.12-03-00810.1992
Grillner, S. and El Manira, A. (2020). Current principles of motor control, with special reference to vertebrate locomotion. *Physiol. Rev.* **100**, 271-320. doi:10.1152/physrev.00015.2019
Gunaydin, L. A., Grosenick, L., Finkelstein, J. C., Kauvar, I. V., Fenno, L. E., Adhikari, A., Lammel, S., Mirzabekov, J. J., Airan, R. D., Zalocusky, K. A. et al. (2014). Natural neural projection dynamics underlying social behavior. *Cell* **157**, 1535-1551. doi:10.1016/j.cell.2014.05.017
Hägglund, M., Borgius, L., Dougherty, K. J. Kiehn, O. (2010). Activation of groups of excitatory neurons in the mammalian spinal cord or hindbrain evokes locomotion. *Nat. Neurosci.* **13**, 246-252. doi:10.1038/nn.2482
Hedrich, U. B. S., Diehl, F. and Stein, W. (2011). Gastric and pyloric motor pattern control by a modulatory projection neuron in the intact crab *Cancer pagurus*. *J. Neurophysiol.* **105**, 1671-1680. doi:10.1152/jn.01105.2010
Hedrich, U. B. S., Smarandache, C. R. and Stein, W. (2009). Differential activation of projection neurons by two sensory pathways contributes to motor pattern selection. *J. Neurophysiol.* **102**, 2866-2879. doi:10.1152/jn.00618.2009
Heinzel, H. G. (1988). Gastric mill activity in the lobster. I. Spontaneous modes of chewing. *J. Neurophysiol.* **59**, 528-550. doi:10.1152/jn.1988.59.2.528
Heinzel, H. G., Weimann, J. M. and Marder, E. (1993). The behavioral repertoire of the gastric mill in the crab, *Cancer pagurus*: an *in situ* endoscopic and electrophysiological examination. *J. Neurosci.* **13**, 1793-1803. doi:10.1523/JNEUROSCI.13-04-01793.1993
Hooper, S. L., Moulins, M. and Nonnotte, L. (1990). Sensory input induces long-lasting changes in the output of the lobster pyloric network. *J. Neurophysiol.* **64**, 1555-1573. doi:10.1152/jn.1990.64.5.1555
Hurwitz, I., Susswein, A. J. and Weiss, K. R. (2005). Transforming tonic firing into a rhythmic output in the *Aplysia* feeding system: presynaptic inhibition of a command-like neuron by a CPG element. *J. Neurophysiol.* **93**, 829-842. doi:10.1152/jn.00559.2004
Jeanne, J. M. and Wilson, R. I. (2015). Convergence, divergence, and reconvergence in a feedforward network improves neural speed and accuracy. *Neuron* **88**, 1014-1026. doi:10.1016/j.neuron.2015.10.018
Jing, J., Sasaki, K., Perkins, M. H., Siniscalchi, M. J., Ludwar, B. C., Cropper, E. C. and Weiss, K. R. (2011). Coordination of distinct motor structures through remote axonal coupling of projection interneurons. *J. Neurosci.* **31**, 15438-15449. doi:10.1523/JNEUROSCI.3741-11.2011
Katz, P. S., Eigg, M. H. and Harris-Warrick, R. M. (1989). Serotonergic/cholinergic muscle receptor cells in the crab stomatogastric nervous system. I. Identification and characterization of the gastropyloric receptor cells. *J. Neurophysiol.* **62**, 558-570. doi:10.1152/jn.1989.62.2.558
Kirby, M. S. and Nusbaum, M. P. (2007). Peptide hormone modulation of a neuronally modulated motor circuit. *J. Neurophysiol.* **98**, 3206-3220. doi:10.1152/jn.00795.2006
Krieger, P., El Manira, A. and Grillner, S. (1996). Activation of pharmacologically distinct metabotropic glutamate receptors depresses reticulospinal-evoked monosynaptic EPSPs in the lamprey spinal cord. *J. Neurophysiol.* **76**, 3834-3841. doi:10.1152/jn.1996.76.6.3834
Lammel, S., Ion, D. I., Roeper, J. and Malenka, R. C. (2011). Projection-specific modulation of dopamine neuron synapses by aversive and rewarding stimuli. *Neuron* **70**, 855-862. doi:10.1016/j.neuron.2011.03.025
Li, W.-C. and Soffe, S. R. (2019). Stimulation of single, possible CHX10 hindbrain neurons turns swimming on and off in young *Xenopus* tadpoles. *Front. Cell .Neurosci.* **13**, 47. doi:10.3389/fncel.2019.00047
Li, H., Horns, F., Wu, B., Xie, Q., Li, J., Li, T., Luginbuhl, D. J., Quake, S. R. and Luo, L. (2017). Classifying *Drosophila* olfactory projection neuron subtypes by single-cell RNA sequencing. *Cell* **171**, 1206-1220.e22. doi:10.1016/j.cell.2017.10.019
Liu, X., Porteous, R., d'Anglemont de Tassigny, X., Colledge, W. H., Millar, R., Petersen, S. L. and Herbison, A. E. (2011). Frequency-dependent recruitment of fast amino acid and slow neuropeptide neurotransmitter release controls gonadotropin-releasing hormone neuron excitability. *J. Neurosci.* **31**, 2421-2430. doi:10.1523/JNEUROSCI.5759-10.2011
Luo, S. X., Huang, J., Li, Q., Mohammad, H., Lee, C.-Y., Krishna, K., Kok, A. M.-Y., Tan, Y. L., Lim, J. Y., Li, H. et al. (2018). Regulation of feeding by somatostatin neurons in the tuberal nucleus. *Science* **361**, 76-81. doi:10.1126/science.aar4983
Marder, E. (2012). Neuromodulation of neuronal circuits: back to the future. *Neuron* **76**, 1-11. doi:10.1016/j.neuron.2012.09.010
Marder, E. and Bucher, D. (2001). Central pattern generators and the control of rhythmic movements. *Curr. Biol.* **11**, R986-R996. doi:10.1016/S0960-9822(01)00581-4
Marder, E. and Bucher, D. (2007). Understanding circuit dynamics using the stomatogastric nervous system of lobsters and crabs. *Annu. Rev. Physiol.* **69**, 291-316. doi:10.1146/annurev.physiol.69.031905.161516
Marder, E., Gutierrez, G. J. and Nusbaum, M. P. (2017). Complicating connectomes: electrical coupling creates parallel pathways and degenerate circuit mechanisms. *Dev. Neurobiol.* **77**, 597-609. doi:10.1002/dneu.22410
McGann, J. P. (2013). Presynaptic inhibition of olfactory sensory neurons: new mechanisms and potential functions. *Chem. Senses.* **38**, 459-474. doi:10.1093/chemse/bjt018

Mesce, K. A., Esch, T. and Kristan, W. B., Jr (2008). Cellular substrates of action selection: a cluster of higher-order descending neurons shapes body posture and locomotion. *J. Comp. Physiol. A Neuroethol. Sens. Neural Behav. Physiol.* **194**, 469-481. doi:10.1007/s00359-008-0319-1

Norris, B. J., Coleman, M. J. and Nusbaum, M. P. (1994). Recruitment of a projection neuron determines gastric mill motor pattern selection in the stomatogastric nervous system of the crab, *Cancer borealis*. *J. Neurophysiol.* **72**, 1451-1463. doi:10.1152/jn.1994.72.4.1451

Norris, B. J., Coleman, M. J. and Nusbaum, M. P. (1996). Pyloric motor pattern modification by a newly identified projection neuron in the crab stomatogastric nervous system. *J. Neurophysiol.* **75**, 97-108. doi:10.1152/jn.1996.75.1.97

Nusbaum, M. P. (1994). Presynaptic control of neurones in pattern-generating networks. *Curr. Opin. Neurobiol.* **4**, 909-914. doi:10.1016/0959-4388(94)90141-4

Nusbaum, M. P., Blitz, D. M. and Marder, E. (2017). Functional consequences of neuropeptide and small-molecule co-transmission. *Nat. Rev. Neurosci.* **18**, 389-403. doi:10.1038/nrn.2017.56

Peng, Y. Y. and Horn, J. P. (1991). Continuous repetitive stimuli are more effective than bursts for evoking LHRH release in bullfrog sympathetic ganglia. *J. Neurosci.* **11**, 85-95. doi:10.1523/JNEUROSCI.11-01-00085.1991

Peng, Y.-Y. and Zucker, R. S. (1993). Release of LHRH is linearly related to the time integral of presynaptic Ca^{2+} elevation above a threshold level in bullfrog sympathetic ganglia. *Neuron* **10**, 465-473. doi:10.1016/0896-6273(93)90334-N

Poels, J., Birse, R. T., Nachman, R. J., Fichna, J., Janecka, A., Vanden Broeck, J. and Nässel, D. R. (2009). Characterization and distribution of NKD, a receptor for *Drosophila* tachykinin-related peptide 6. *Peptides* **30**, 545-556. doi:10.1016/j.peptides.2008.10.012

Poels, J., Verlinden, H., Fichna, J., Van Loy, T., Franssens, V., Studzian, K., Janecka, A., Nachman, R. J. and Vanden Broeck, J. (2007). Functional comparison of two evolutionary conserved insect neurokinin-like receptors. *Peptides* **28**, 103-108. doi:10.1016/j.peptides.2006.06.014

Puhl, J. G., Bigelow, A. W., Rue, M. C. P. and Mesce, K. A. (2018). Functional recovery of a locomotor network after injury: plasticity beyond the central nervous system. *eNeuro* **5**, eneuro0195-118. doi:10.1523/ENEURO.0195-18.2018

Puhl, J. G., Masino, M. A. and Mesce, K. A. (2012). Necessary, sufficient and permissive: a single locomotor command neuron important for intersegmental coordination. *J. Neurosci.* **32**, 17646-17657. doi:10.1523/JNEUROSCI.2249-12.2012

Qiu, J., Nestor, C. C., Zhang, C., Padilla, S. L., Palmiter, R. D., Kelly, M. J. and Rønnekleiv, O. K. (2016). High-frequency stimulation-induced peptide release synchronizes arcuate kisspeptin neurons and excites GnRH neurons. *eLife* **5**, e16246. doi:10.7554/eLife.16246.016

Rodriguez, J. C., Blitz, D. M. and Nusbaum, M. P. (2013). Convergent rhythm generation from divergent cellular mechanisms. *J. Neurosci.* **33**, 18047-18064. doi:10.1523/JNEUROSCI.3217-13.2013

Rosen, S. C., Teyke, T., Miller, M. W., Weiss, K. R. and Kupfermann, I. (1991). Identification and characterization of cerebral-to-buccal interneurons implicated in the control of motor programs associated with feeding in *Aplysia*. *J. Neurosci.* **11**, 3630-3655. doi:10.1523/JNEUROSCI.11-11-03630.1991

Ruder, L. and Arber, S. (2019). Brainstem circuits controlling action diversification. *Annu. Rev. Neurosci.* **42**, 485-504. doi:10.1146/annurev-neuro-070918-050201

Saideman, S. R., Blitz, D. M. and Nusbaum, M. P. (2007). Convergent motor patterns from divergent circuits. *J. Neurosci.* **27**, 6664-6674. doi:10.1523/JNEUROSCI.0315-07.2007

Saideman, S. R., Christie, A. E., Torfs, P., Huybrechts, J., Schoofs, L. and Nusbaum, M. P. (2006). Actions of kinin peptides in the stomatogastric ganglion of the crab *Cancer borealis*. *J. Exp. Biol.* **209**, 3664-3676. doi:10.1242/jeb.02415

Sakurai, A. and Katz, P. S. (2009). Functional recovery after lesion of a central pattern generator. *J. Neurosci.* **29**, 13115-13125. doi:10.1523/JNEUROSCI.3485-09.2009

Sakurai, A., Tamvacakis, A. N. and Katz, P. S. (2016). Recruitment of polysynaptic connections underlies functional recovery of a neural circuit after lesion. *eNeuro* **3**, 0056-0016. doi:10.1523/ENEURO.0056-16.2016

Sánchez, J. A. D., Li, Y. and Kirk, M. D. (2000). Regeneration of cerebral-buccal interneurons and recovery of ingestion buccal motor programs in *Aplysia* after CNS lesions. *J. Neurophysiol.* **84**, 2961-2974. doi:10.1152/jn.2000.84.6.2961

Selverston, A. I. and Miller, J. P. (1980). Mechanisms underlying pattern generation in lobster stomatogastric ganglion as determined by selective inactivation of identified neurons. I. Pyloric system. *J. Neurophysiol.* **44**, 1102-1121. doi:10.1152/jn.1980.44.6.1102

Shimazaki, T., Tanimoto, M., Oda, Y. and Higashijima, S.-I. (2019). Behavioral role of the reciprocal inhibition between a pair of Mauthner cells during fast escapes in zebrafish. *J. Neurosci.* **39**, 1182-1194. doi:10.1523/JNEUROSCI.1964-18.2018

Sillar, K. T. and Simmers, A. J. (1994). Presynaptic inhibition of primary afferent transmitter release by 5-hydroxytryptamine at a mechanosensory synapse in the vertebrate spinal cord. *J. Neurosci.* **14**, 2636-2647. doi:10.1523/JNEUROSCI.14-05-02636.1994

Simmers, J. and Moulins, M. (1988). A disynaptic sensorimotor pathway in the lobster stomatogastric system. *J. Neurophysiol.* **59**, 740-756. doi:10.1152/jn.1988.59.3.740

Sirois, J., Frigon, A. and Gossard, J.-P. (2013). Independent control of presynaptic inhibition by reticulospinal and sensory inputs at rest and during rhythmic activities in the cat. *J. Neurosci.* **33**, 8055-8067. doi:10.1523/JNEUROSCI.2911-12.2013

Smarandache, C. R. and Stein, W. (2007). Sensory-induced modification of two motor patterns in the crab, *Cancer pagurus*. *J. Exp. Biol.* **210**, 2912-2922. doi:10.1242/jeb.006874

Stein, W. (2017). Stomatogastric nervous system. *Oxf. Res. Encycl. Neurosci.* doi:10.1093/acrefore/9780190264086.013.153

Stein, W., DeLong, N. D., Wood, D. E. and Nusbaum, M. P. (2007). Divergent co-transmitter actions underlie motor pattern activation by a modulatory projection neuron. *Eur. J. Neurosci.* **26**, 1148-1165. doi:10.1111/j.1460-9568.2007.05744.x

Stein, W., Smarandache, C. R., Nickmann, M. and Hedrich, U. B. (2006). Functional consequences of activity-dependent synaptic enhancement at a crustacean neuromuscular junction. *J. Exp. Biol.* **209**, 1285-1300. doi:10.1242/jeb.02133

Svensson, E., Apergis-Schoute, J., Burnstock, G., Nusbaum, M. P., Parker, D. and Schiöth, H. B. (2019). General principles of neuronal co-transmission: insights from multiple model systems. *Front. Neural Circuits* **12**, 117. doi:10.3389/fncir.2018.00117

Swensen, A. M. and Marder, E. (2000). Multiple peptides converge to activate the same voltage-dependent current in a central pattern-generating circuit. *J. Neurosci.* **20**, 6752-6759. doi:10.1523/JNEUROSCI.20-18-06752.2000

Swensen, A. M. and Marder, E. (2001). Modulators with convergent cellular actions elicit distinct circuit outputs. *J. Neurosci.* **21**, 4050-4058. doi:10.1523/JNEUROSCI.21-11-04050.2001

Takahashi, M. and Alford, S. (2002). The requirement of presynaptic metabotropic glutamate receptors for the maintenance of locomotion. *J. Neurosci.* **22**, 3692-3699. doi:10.1523/JNEUROSCI.22-09-03692.2002

van den Pol, A. N. (2012). Neuropeptide transmission in brain circuits. *Neuron* **76**, 98-115. doi:10.1016/j.neuron.2012.09.014

Vilim, F. S., Cropper, E. C., Price, D. A., Kupfermann, I. and Weiss, K. R. (1996). Release of peptide cotransmitters in *Aplysia*: regulation and functional implications. *J. Neurosci.* **16**, 8105-8114. doi:10.1523/JNEUROSCI.16-24-08105.1996

Vilim, F. S., Cropper, E. C., Price, D. A., Kupfermann, I. and Weiss, K. R. (2000). Peptide cotransmitter release from motorneuron B16 in *Aplysia californica*: costorage, corelease, and functional implications. *J. Neurosci.* **20**, 2036-2042. doi:10.1523/JNEUROSCI.20-05-02036.2000

Wang, J. W. (2012). Presynaptic modulation of early olfactory processing in *Drosophila*. *Dev. Neurobiol.* **72**, 87-99. doi:10.1002/dneu.20936

Weeks, J. C. and Kristan, W. B., Jr. (1978). Initiation, maintenance and modulation of swimming in the medicinal leech by the activity of a single neurone. *J. Exp. Biol.* **77**, 71-88.

Weimann, J. M., Meyrand, P. and Marder, E. (1991). Neurons that form multiple pattern generators: identification and multiple activity patterns of gastric/pyloric neurons in the crab stomatogastric system. *J. Neurophysiol.* **65**, 111-122. doi:10.1152/jn.1991.65.1.111

Westberg, K.-G., Kolta, A., Clavelou, P., Sandström, G. and Lund, J. P. (2000). Evidence for functional compartmentalization of trigeminal muscle spindle afferents during fictive mastication in the rabbit. *Eur. J. Neurosci.* **12**, 1145-1154. doi:10.1046/j.1460-9568.2000.00001.x

Whim, M. D. and Lloyd, P. E. (1989). Frequency-dependent release of peptide cotransmitters from identified cholinergic motor neurons in *Aplysia*. *Proc. Natl. Acad. Sci. USA* **86**, 9034-9038. doi:10.1073/pnas.86.22.9034

Whim, M. D. and Lloyd, P. E. (1994). Differential regulation of the release of the same peptide transmitters from individual identified motor neurons in culture. *J. Neurosci.* **14**, 4244-4251. doi:10.1523/JNEUROSCI.14-07-04244.1994

White, R. S. and Nusbaum, M. P. (2011). The same core rhythm generator underlies different rhythmic motor patterns. *J. Neurosci.* **31**, 11484-11494. doi:10.1523/JNEUROSCI.1885-11.2011

White, R. S., Spencer, R. M., Nusbaum, M. P. and Blitz, D. M. (2017). State-dependent sensorimotor gating in a rhythmic motor system. *J. Neurophysiol.* **118**, 2806-2818. doi:10.1152/jn.00420.2017

Wolf, H. and Pearson, K. G. (1988). Proprioceptive input patterns elevator activity in the locust flight system. *J. Neurophysiol.* **59**, 1831-1853. doi:10.1152/jn.1988.59.6.1831

Wood, D. E., Manor, Y., Nadim, F. and Nusbaum, M. P. (2004). Intercircuit control via rhythmic regulation of projection neuron activity. *J. Neurosci.* **24**, 7455-7463. doi:10.1523/JNEUROSCI.1840-04.2004

Wood, D. E., Stein, W. and Nusbaum, M. P. (2000). Projection neurons with shared cotransmitters elicit different motor patterns from the same neural circuit. *J. Neurosci.* **20**, 8943-8953. doi:10.1523/JNEUROSCI.20-23-08943.2000